OCEANIC MANTLE PHASES RECORDED ON HYDROPHONES AND SEISMOGRAPHS IN THE NORTHWESTERN PACIFIC AT DISTANCES BETWEEN 7° AND 40°

A DISSERTATION SUBMITTED TO THE GRADUATE DIVISION OF THE
UNIVERSITY OF HAWAII IN PARTIAL FULFILLMENT
OF THE REQUIREMENTS FOR THE DEGREE OF

DOCTOR OF PHILOSOPHY

IN GEOSCIENCES - SOLID EARTH GEOPHYSICS

MAY 1971

By

Daniel Alvin Walker

Dissertation Committee:

George H. Sutton, Chairman
Doak C. Cox
Augustine S. Furumoto
Gordon A. Macdonald
Ralph M. Moberly, Jr.

ABSTRACT

Body-wave data from 60 earthquakes recorded on hydrophones (recorded frequencies of 3 to 8 Hz) at Midway, Wake, and Eniwetok and from 100 earthquakes recorded on seismographs (recorded frequencies of 0.3 to 3 Hz) at Midway, Wake, and Marcus indicate the following for the Northwestern Pacific Basin area: Observed times of P-wave arrivals on hydrophones compared to the expected times of arrivals of the normal refracted mantle P phases are early (usually by several seconds) for distances of 9°.4 to 19°.5, late (by as much as 64 sec) for distances of 19°.5 to 33°.1, and on time for distances of 33°.1 to 39°.8; observed times of S-wave arrivals on hydrophones compared to the expected times of arrivals of the normal refracted mantle S phases are early (by as much as 34 sec) for distances of 9°.4 to 20°.8, late for distances of 20°.8 to 32°.9, and no data is available for distances beyond 32°.9; observed times of P-wave arrivals on seismographs are early for shallow events and on time for deeper events for distances of 7°.59 to 23°, and on time for distances of 23° to 39°.10; and, observed times of S-wave arrivals on seismographs are very early (by as much as 23 sec) for distances of 7°.59 to 20°.34, and on time for distances of 20°.34 to 39°.10.

Similar data from 25 earthquakes recorded on hydrophones and from 39 earthquakes recorded on seismographs indicate the following for the East Caroline Basin-Ontong Java Plateau-Nauru Sea area: Observed times of P-wave arrivals on hydrophones are on time for distances of 16°.4 to 18°.3, late for distances of 18°.3 to 22°.2, and on time for distances of 22°.2 to 39°.6; S-wave arrivals on hydrophones are unclear or not apparent for distances of 16°.4 to 39°.6; P-wave arrivals on seismographs are

slightly late for distances of 15°.98 to 39°.88; and, S-wave arrivals on seismographs are on time for the few instances in which they were well recorded (at 23°.61, 32°.25, 33°.80, and 37°.86).

These observations and additional analyses of the travel-time data suggest the following for the mantle under the Northwestern Pacific Basin: a zone of low P-wave velocity with a thickness of about 75 km beginning in the uppermost 100 km of the earth, perhaps very close to the M discontinuity; a waveguide immediately below the M discontinuity which propagates 3 to 8 Hz energy of compressional and shear waves with velocities of 8.28±0.03 and 4.79±0.04 km/sec, respectively, to great distances (observed to 33°, with the waveguide for compressional waves being considerably more efficient than the waveguide for shear waves); and, an asthenosphere of low Q for frequencies of 3 to 8 Hz compared to that for material above and below.

Similar considerations suggest the following for the mantle under the East Caroline Basin-Ontong Java Plateau-Nauru Sea: a waveguide immediately below the M discontinuity which propagates 3 to 8 Hz energy of compressional waves with a velocity of 8.47±0.48 km/sec to at least 22°; a weaker waveguide for shear waves than observed for the area to the north; an asthenosphere of low Q for frequencies of 3 to 8 Hz compared to that for material above and below; and, a velocity distribution somewhat different from that for the area to the north since, for normal refracted mantle P phases recorded in the distance range of 22° to 40°, travel time residuals are generally slightly negative for the area to the north and slightly positive for the area to the south.

TABLE OF CONTENTS

LIST OF TABLES

LIST OF FIGURES

1. INTRODUCTION

Background

Because of the distribution of seismic zones and recording stations on the earth's surface, most body-wave travel-time data in the 10° to 30° epicentral distance range is obtained by continental seismic stations which record earthquake waves from continental seismic belts or from nearby island arcs. In other words, there are few seismic stations out in the oceans in the distance range of 10° to 30° away from zones of seismicity, and it is body-wave data in this distance range which provides the most information on P- and S-wave velocities in the uppermost 300 or 400 km of the earth. Thus, any mantle velocities determined from the available body-wave data are probably more representative of continental or transitional mantle structure than of oceanic - if such differences do, in fact, exist. Data in this distance range are available for such oceanic regions as the Philippine Sea and the New Hebrides-Fiji-Tonga-Samoa area, but whether the mantle in these regions should be considered as oceanic, continental, or some mixture of both is not yet certain. Comprehensive body-wave travel-time studies for the regions most likely to have a purely oceanic mantle, the deep ocean basins, are not available because few island seismic stations are so located that travel paths for earthquakes at epicentral distances in the range of 10° to 30° from the island seismic stations would be in the mantle underlying the deep ocean basins. Consequently, our present knowledge of ocean-basin mantle-velocity structures is based primarily on surface-wave studies which mainly provide information on shear-velocity distribution. In the absence of body-wave data a potentially

significant void in our knowledge is apparent since the deep ocean basins overlie a considerable portion of the earth's mantle. This omission is made more conspicuous by current efforts, brought about by such concepts as sea-floor spreading and plate tectonics, to determine deep processes in the oceanic mantle.

Historical Development

The author's direct involvement in efforts to obtain velocity models for the oceanic mantle began at the Hawaii Institute of Geophysics (HIG) of the University of Hawaii in the fall of 1963. In studying Pacific Missile Range hydrophone records, the author noticed that hydrophones at Midway, Wake, and Eniwetok were recording compressional and shear phases from earthquakes in the portion of the circum-Pacific arc that extends from the Aleutian Islands to the Solomon Islands. An unusual thing about the times of arrivals was that, for distances of 20° to 33°, they were very much later (as much as 64 sec) than the expected times (Jeffreys and Bullen, 1958) of arrivals for the normal refracted mantle phases. This observation served to impress the author with the fact that seismologists had been unable to give adequate attention to a very important part of the earth because of the distribution of seismic zones and stations; namely, the mantle underlying the deep ocean basins. It was then decided that a significant contribution to the field would be made if body-wave data were obtained for what could be considered a purely oceanic mantle. This is the basic idea which the author had in 1963 and this idea provided the motivation for his work at HIG since that time.

The idea was discussed with Dr. Furumoto of HIG and a proposal to the National Science Foundation (NSF) to install seismic stations on

Midway, Wake, and Marcus islands was written by Drs. Woollard, Furumoto, and Adams (all of HIG). The objective of the proposed research was to conduct a seismological investigation of the mantle underlying the Northwestern Pacific Basin. The proposal was approved beginning in the fall of 1964 and tape recording seismographs were designed by W. M. Adams and G. L. Maynard (a member of the staff of HIG). Tape systems were chosen for several reasons: (a) the cost was much less than using photographic recorders and was comparable to hot-pen recorders, (b) assistance of local personnel was required only on a once-a-month basis rather than a daily basis, and (c) tape recording offered advantages in data analysis that are not inherent in visual recordings. The tape systems were placed at the island sites by 1965. The installations were made by A. S. Furumoto, W. M. Adams, G. L. Maynard, and this author. Also in 1965, the author received his M.S. in Geosciences with a thesis entitled "A Study of the Northwestern Pacific Upper Mantle." The preliminary interpretation that the observed phases were normal refracted mantle phases as given in that thesis was shown to be erroneous by subsequent information which will be presented in this dissertation. Out on the island sites, the tape systems were encountering several serious problems: (a) adverse environmental conditions (high humidity, temperatures, and salinity) caused continual fouling of the tape recorder heads, (b) local personnel were unable to monitor and compensate for unexpectedly large changes in noise level, (c) T phases and microseism storms were continually saturating the amplifiers, and (d) frequent power failures on the order of seconds or minutes destroyed timing precision. The author continued studying hydrophone arrivals and began work on a

computer program that could be used to derive velocity models of the earth from observed body-wave data.

In 1967, a new proposal to NSF was written by Drs. Sutton (also of HIG) and Furumoto to design a new instrumentation system which would eliminate the problems encountered with the tape systems and to continue operation of the island stations. The proposal was approved. The improved instrumentation uses a solid state double-pen recorder with its own emergency power supply. The two channels are used to record a short-period vertical (SPZ) Hall-Sears 10-1 geophone and a long-period vertical (LPZ) Sprengnether seismometer. The magnification of the SPZ is a maximum at approximately 0.6 sec and the magnification of the LPZ is a maximum at approximately 15 sec. Detailed response curves are published elsewhere (Sutton and Walker, 1970). In 1968, a paper by this author and Dr. Sutton entitled "The Agreement of Proposed Earth Models with Observed Body-Wave Travel Times" was published in the Bulletin of the Seismological Society of America. The computer program described in this paper was the tool needed to derive mantle models when, and if, an adequate body of data was accumulated; however, data obtained by the double-pen recorders were coming in at a very slow rate.

In January of 1969, another proposal to NSF was written by this author to continue operation of the Northwestern Pacific Island Stations and to expand the network to the South Pacific. The proposal was partially approved. Also in 1969, all hydrophone data was evaluated, and these data with their interpretations are presented as Part II of the dissertation. Since 1969, the author has worked on the installation of a seismic station on Easter Island in the South Pacific and on the

evaluation of seismograph data from the Northwestern Pacific stations. This evaluation has been completed and these data with their interpretations are presented in Part III of the dissertation.

Format

The reason for the presentation of the data with their interpretations in two parts (Part II and Part III) is mostly historical (the hydrophone data were evaluated before an acceptable body of seismograph data were accumulated), although there is also reason to believe that independent evaluations of the hydrophone and seismograph data, prior to any combined evaluation, are the best means of arriving at a proper interpretation of the combined data.

In Part II, 100 compressional-wave arrivals and 49 shear-wave arrivals from 87 earthquakes having epicentral distances ranging from 9°.4 to 39°.8 as recorded on hydrophones at Midway, Wake, and Eniwetok are studied. Most of the earthquakes occurred in the portion of the circum-Pacific belt that extends from the Aleutian Islands down through the Solomon Islands (Figure 1). Examination of the raw data showed that travel times for earthquakes south of Guam were anomalous with respect to the rest of the observations. For this reason, 12° north latitude was chosen somewhat arbitrarily as the dividing line (dashed line in Figure 1). Bathymetry indicates that the travel paths of seismic waves from earthquakes occurring south of Guam would be under the shallower East Caroline Basin-Ontong Java Plateau-Nauru Sea area, as well as under the Northwestern Pacific Basin. Thus, travel-time data for events north of Guam could be considered as indicative of pure oceanic mantle structure, whereas the data for events south of Guam might be indicative

of a somewhat different oceanic mantle structure. For this reason, the data and the discussions of the data are presented separately for the areas north and south of 12° north latitude.

In Part III, 135 compressional-wave arrivals and 67 shear-wave arrivals from 139 earthquakes having epicentral distances ranging from 7°.59 to 39°.88 as recorded on short- and long-period vertical seismographs at Midway, Wake, and Marcus islands are discussed. As in Part II, most of the earthquakes occurred in the portion of the circum-Pacific belt that extends from the Aleutian Islands down through the Solomon Islands; and the data are examined separately for events north and south of 12° north latitude representing the deep Northwestern Pacific Basin and the shallower East Caroline Basin-Ontong Java Plateau-Nauru Sea area, respectively. In each of the discussions (north and south of 12° north latitude) of Part III, interpretations of the seismograph data are given first; and then interpretations of the combined hydrophone and seismograph data are presented.

Other Studies

Consideration is now given to the available direct and indirect evidence concerning the structure of the mantle underlying the Northwestern Pacific Basin and the East Caroline Basin-Ontong Java Plateau-Nauru Sea area.

In a study of travel times for Pacific nuclear explosions using the results of Carder and Bailey (1958) and additional data personally given to him by Carder, Jeffreys (1962) determined that differences between observed P-wave travel times and expected P-wave travel times (Jeffreys and Bullen, 1958) for distances of 5°, 10°, 15°, and 20° would be -5.7,

-7.3, -6.0 and -2.1 sec, respectively. These values were based on the observed travel times of P phases from nuclear detonations near Bikini and Eniwetok to permanent seismic stations on Guam and Truk and to temporary seismic stations on Kwajalein and Wake. In the distance ranges of 3°.3 to 3°.6, 7°.7 to 8°.7, 11°.0 to 13°.9, 17°.1 to 18°.6, and 20°.1 to 20°.5, the number of observed P phases are 2, 2, 4, 5, and 5, respectively, giving a total of 18 P phases observed between 3°.3 and 20°.5. Similar studies by Doyle and Webb (1963) of P travel times from Bikini and Eniwetok to an Australian station on Rabaul revealed observed minus expected travel times of -9.1, -8.4, -9.1, and -9.1 sec for distances of 19°.11, 19°.22, 21°.12 and 21°.21, respectively.

Of the 22 P phases observed, only 2 had travel paths north of 12° north latitude. These phases were recorded at Wake from tests at Bikini and at Eniwetok at epicentral distances of 7°.7 and 8°.7, respectively. Data for similar travel paths are not available from this dissertation, but data for similar epicentral distances (earthquakes from the Mariana Islands recorded at Marcus) are available. Observed minus expected travel times at Wake were -6 to -7 sec while for comparable distances observed minus expected travel times at Marcus were -3 to -8 sec. It is not yet known what significance should be given to the similarity of these data.

Fifteen of the 22 P phases observed had travel paths south of 12° north latitude. These phases were recorded at Bikini, Kwajalein, Truk, and Rabaul. The remaining 5 P phases had travel paths which were partly north and partly south of 12° north latitude. These 5 phases were recorded on Guam at distances of 17°.1, 17°.1, 20°.1, 20°.2, and 20°.2.

Observed minus expected travel times for all 20 of these phases were in the range of -9 to -2 sec. These data and data for similar travel paths available from this dissertation are discussed in Parts II and III under "Discussion (Events South of 12° North Latitude)."

Evidence concerning the structure of the oceanic mantle may be obtained from long-period oceanic surface-wave data. Such a study by Press (1969), utilizing Monte Carlo inversion techniques, indicated a low-velocity zone for shear waves beginning at a depth of about 100 km with its center at depths between 150 and 250 km. Since a similar study (Press, 1968), using generalized long-period surface-wave data (no distinction was made for oceanic, continental, or transitional data), suggested somewhat similar velocity distributions, it is not certain whether significant differences in oceanic and continental mantle structures are indicated by these long-period surface-wave data. Part of the problem may be due to the fact that in the Monte Carlo method, body-wave data are used to constrain the possible solutions; and, if the body-wave data used are not representative of actual oceanic body-wave data, the possible solutions would be improperly constrained and the resulting velocity models might not actually represent an oceanic mantle.

Differences between continental and oceanic mantle structure are, perhaps, best suggested by the general equivalence of heat flow data for continents and oceans and by concepts of sea-floor spreading. Since most of the heat flow observed on the earth's surface is due to radioactive material in the crust, and since the continents have a considerably thicker crust than the oceans, it was thought that the heat flow of continents should be considerably higher than the heat flow of

oceans. Actual measurements showed that this was not the case, and the logical conclusion of this observation is that the continental and oceanic mantles are different. Differences are also implicit in the concept that crust is created at oceanic rises, carried to regions of subsidence (continental margins), thrust under continents, assimilated into the asthenosphere or mesosphere, and, perhaps, recycled back to the oceanic rise.

II. HYDROPHONE ARRIVALS

Data (Events North of 12° North Latitude)

U.S. Coast and Geodetic Survey epicentral data are listed in Table 1 and observed travel times and residuals (observed minus expected travel times) are given in Table 2. Expected travel times are taken from the Jeffreys-Bullen (J-B) tables (1958). Ten of the 71 log, power-level recordings of hydrophone arrivals are presented in Figure 2 and all others are available from this author on request.

The J-B tables were used in preference to the Herrin (1968) tables for the following reasons: Prior to 1968, when these studies began, the J-B tables were generally recognized as the standard reference for the travel times of seismic waves; and, unlike the J-B tables, the Herrin tables do not include travel times for shear phases, and a good portion of this investigation is concerned with the travel times of these phases. For those wishing to compare the observed P-wave travel-time data with the P-wave travel times of the Herrin tables rather than the J-B tables, the following information is provided: for epicentral distances of 5°, 10°, 15°, 20°, 25°, 30°, 35°, 40° and for a focal depth of 0 km, the P-wave travel times of the Herrin tables are less than the P-wave travel times of the J-B tables by approximately 3.8, 3.5, 3.7, 2.4, 3.0, 2.8, and 2.4 sec, respectively; and, for similar epicentral distances and for a focal depth of 100 km, the Herrin times are less by 2.7, 2.8, 2.9, 2.5, 3.0, 2.7, and 2.3 sec, respectively. Had P-wave travel time residuals been computed with reference to the Herrin tables rather than the J-B tables, Herrin P-wave travel time residuals would be more positive than the J-B P-wave travel time residuals by approximately 2 to

4 sec - with the actual value depending on the epicentral distance and the focal depth. It should be noted, however, that for distances of less than 20° the travel times of the Herrin tables are representative of a velocity distribution for the upper mantle having travel times consistent with observed travel times in the central United States.

The residuals (Table 2) indicate that observed compressional phases in the 9°.4 to 19°.5 distance range (arrivals 1 through 37) arrived sooner than the expected J-B P phases, as was likewise true for the observed shear phases in the 9°.4 to 20°.8 range (arrivals 1 through 41). The large positive compressional-wave residual of 11.0 sec and the slightly positive shear-wave residual of 1.3 sec for arrival 18 is the most notable exception, and is possibly related to the fact that arrival 18 had the deepest focal depth (214 km). Observed compressional phases in the 19°.5 to 33°.1 range (arrivals 37 through 66) arrived increasingly later than the expected J-B P phases, as did also the observed shear phases in the 20°.8 to 32°.9 range (arrivals 41 through 65). In this second (slower) group of arrivals, the small negative P residual of 0.5 sec for arrival 61, at a distance of 29°.0, appears as the most notable exception. Again focal depth may be significant in that arrival 61 had the deepest focal depth (382 km). Arrival times of observed compressional waves beyond 33°.1 were similar to the J-B P arrival times and no later phases were observed. Shear waves have not been observed for epicentral distances beyond 32°.9. Fifteen compressional waves have been observed for events beyond 40° (not given here); all had arrival times which were in good agreement with the arrival times of the J-B P phases and no later phases were observed.

Phases in the first group (1 through 37), where arrival times were early, came from events in the Mariana Islands that were recorded mostly at Eniwetok. Neither Wake nor Midway is as close as Eniwetok to the circum-Pacific belt. Phases in the second group (38 through 66), where arrival times were increasingly late, came from events occurring north of the Mariana Islands. These events were recorded at all three stations. A map showing the location of those events having P-phase arrival times later than the expected arrival times by more than 10.0 sec at the three stations is given in Figure 3. The reader might wonder why an event in the Bonin Islands (e.g., arrival 52) which was recorded at Eniwetok was not recorded at Wake, since epicentral distances appear comparable. The explanation is that all events are not necessarily well recorded at all stations and only the strongest and most distinct recordings were used in this study. Of the 5 arrivals recorded beyond 33°.1 (arrivals 67 through 71), two were produced by events in the Aleutian Islands, and one each by events in the Mariana Islands, the Sea of Japan, and off Taiwan Island. These events were also recorded at all three stations.

Travel-time plots of compressional and shear waves are given in Figures 4 and 5. Inverse slopes of 8.28±0.03 and 4.79±0.04 km/sec were determined from a least squares fit of compressional- and shear-wave travel-time data having focal depths less than 100 km and epicentral distances less than 30°. Intercepts of +1.4 and +7.9 sec were found for the compressional- and shear-wave curves, respectively. The obvious linearity of the travel-time curves out to 30° immediately suggests some sort of guided-wave interpretation.

Discussion (Events North of 12° North Latitude)

The high apparent velocities obtained from the travel-time curves preclude consideration of the observed phases as any crustal phases (p, $\overline{P}$, P*, Pm; also s, $\overline{S}$, S*, and Sm).

Although velocities immediately below the M discontinuity for the oceans are thought to average 8.1 and 4.7 km/sec for compressional and shear waves, respectively (Gutenburg, 1959), compressional velocities as high as 8.6 km/sec have been found immediately below the M discontinuity in the Pacific (Raitt et al., 1969). Therefore, Pn and Sn (or Ph.f. and Sh.f.; Oliver and Isacks, 1967) as possible descriptions of the observed phases would imply higher than normal, but not unusual velocities immediately below the M discontinuity for the Northwestern Pacific. However, if a Pn (Sn) phase interpretation is to be accepted, then the apparent absence of the J-B P phase, even for large-magnitude events at distances from 19°.5 to 33°.1, will have to be explained. Molnar and Oliver (1969) did not consider this when they interpreted as an Sn phase the shear phases at hydrophones which Walker (1965) had reported earlier. A possible explanation, which would support their interpretations, is that, in the distance range in question, lower frequencies may be more predominant in the J-B P phase than beyond 33°.1; and, since the hydrophones record higher frequency phases more readily, the lower frequency J-B P phase is not well recorded in the 19°.5 to 33°.1 range. If this explanation proves valid, further inquiry should be made into the reason for this lack of high-frequency energy and particular attention should be paid to the sudden appearance of the higher frequency J-B P phase beyond 33°.1 and the coincident sudden disappearance of the Pn phase.

Pa and Sa phases, having periods much longer than the J-B P or S phases, have velocities of 8.0 and 4.4 km/sec (Caloi, 1953), respectively. Earlier arriving phases are observed in front of the later-arriving Pa and Sa phases. Hydrophone response to the predominantly lower frequencies of the Pa (Sa) phases would not be as good as to the higher frequencies of the Pn (Sn) phases. In addition, this interpretation would present the same problem as those of a Pn (Sn) phase interpretation.

Another possibility is that the observed phases might be the first-arriving refracted mantle wave. Since the refracted mantle wave usually appears as the clearest arrival on a short-period seismometer, a single phase observed throughout an epicentral distance range of 9°.4 to 39°.8 for events as large as magnitude 8.0 could be interpreted to be a refracted mantle arrival. Using methods described in an earlier paper (Walker and Sutton, 1968), P and S velocity-depth functions having travel times generally in agreement with the observed travel times (RMS error ±5.3 sec for HIG 3 and ±6.0 sec for HIG 4) were found. These unusual models (HIG 3 and HIG 4) are plotted along with the J-B P- and S-velocity models in Figures 6 and 7. A large residual of -33.3 sec from model HIG 3 for the one deep event in the critical distance range (arrival no. 61, h = 382 km, Δ = 29°.0) argues against this interpretation.

Data (Events South of 12° North Latitude)

Coast and Geodetic Survey epicentral data for this region are given in Table 3, travel times and residuals for the arrivals are given in Table 4, and six recordings are presented in Figure 8. The residuals indicate that observed compressional waves in the 16°.4 to 18°.3 range

(arrivals 1 through 5) have arrival times close to the arrival times of the J-B P phase. Observed compressional waves in the 18°.3 to 22°.2 range (arrivals 6 through 16) have arrival times which are later than the arrival times of the J-B P phase. Beyond 22°.2 arrival times are again comparable to the arrival times of the J-B P phase. Most S waves are unclear and in many cases no S waves were found. All the compressional phases shown in Figure 8 have exceptionally distinct onsets and only a single compressional phase was observed on each record. A travel-time plot of compressional-wave data is given in Figure 9. An inverse slope of 8.47±0.48 km/sec was determined from a least squares fit of data for events having focal depths less than 100 km and epicentral distances less than 24°. An intercept of +15.0 sec was found.

Discussion (Events South of 12° North Latitude)

The arguments presented in the discussion of the phases observed for events north of 12° north latitude are applicable here. Interpreting these phases as first-arriving refracted mantle phases, a model (HIG 5) was found (RMS error ±4.3 sec) and is plotted along with the J-B P-velocity model in Figure 10.

As mentioned in Part I, the results of studies by Carder and Bailey (1958), Jeffreys (1962), and Doyle and Webb (1963) indicate negative P-wave travel time residuals (-9 to -2 sec) for this area. These results and the large positive residuals of Table 4 suggest that the normal refracted mantle P phases were not observed on the hydrophones and that a guided P phase was observed on the hydrophones.

III. SEISMOGRAPH ARRIVALS

Data (Events North of 12° North Latitude)

U.S. Coast and Geodetic Survey epicentral data are listed in Table 5 and observed travel times and residuals are given in Table 6. An epicenter map is given in Figure 11. Several short- and long-period seismograms are presented in Figure 12 and copies of all other data are available from this author on request.

Compressional arrivals:

7°59-10°25 (Events #1-17). The frequency of the observed arrivals on the short-period vertical seismograph (SPZ) appears to be the normal frequency of refracted mantle phases (i.e., ≃ 1 Hz). Travel times are generally early for shallow events and "on time," or late, for deeper events. An examination of residuals in relation to their focal depths indicates that events having positive residuals have focal depths greater than 135 km. Observed phases on the long-period vertical seismograph (LPZ) arrive at approximately the same time and appear to have about the same frequency as the SPZ arrivals. No significant phases other than the first arrivals are observed.

10°25-39°10 (Events #18-106). While the SPZ continues to record phases having frequencies of approximately 1 Hz, noticeable lower frequency phases become apparent with increasing distance on the LPZ. Arrival times on both instruments continue to be approximately the same and no significant phases other than the first arrivals are observed. Out to approximately 23° (Events #18-79), times of arrivals from earthquakes of shallow and intermediate depth are generally early. Event 24 with an epicentral distance of 12°31 and a focal depth of

516 km has an anomalously large residual (-21.3 sec) which can be attributed either to a timing error or to an inaccurate hypocenter. The other deep focus events (20, 44, and 76 at epicentral distances of 10°.39, 17°.68, and 21°.81, and with focal depths of 319, 347, and 417 km, respectively) have residuals of 0.0, +0.5, and +3.8 sec, respectively. Beyond 23° (Events #80-106), observed travel times are close to expected values.

Shear arrivals:

7°.59-20°.34 (Events #1-65). On the LPZ it is not certain whether normal long-period S waves are observed. High-frequency S waves (1-2 Hz) observed on the SPZ come in on the LPZ at about the same time. This arrival could obscure any phases of lower frequencies which might be present. Also in this distance range, the strength and frequency of the normal long-period S phase may not be discernible from the background noise of about 3 to 6 seconds period, which often is present. The times of arrivals are generally very early (often as much as 20 seconds), and no other significant phases are observed. The only exceptions are events 8, 10, 15, 16, and 20 having focal depths of 206, 225, 229, 204, and 319 km, respectively. These events do not have significant negative residuals. However, events 6, 9, 11, 12, and 47 with focal depths of 165, 134, 135, 115, and 116 km, respectively, have large negative residuals.

20°.34-39°.10 (Events #66-106). In this distance range the normal long-period S phase makes its appearance as a distinct phase. Beyond 20°.65 (Event #70), the high-frequency S phase is no longer apparent on either the SPZ or the LPZ, and the normal long-period S phase appears

as the first-arriving S wave. The LPZ recording of event #70 (Fig. 12) shows both the high-frequency S phase and the normal long-period S phase.

Discussion (Events North of 12° North Latitude)

The data indicate that the normal refracted mantle P (≃ 1 Hz) appears to be well recorded at all distances on the seismographs. The travel time residuals of the normal refracted mantle P waves suggest higher velocities in the uppermost mantle than in the J-B model, with relatively lower velocities below this region. Using methods described in an earlier paper (Walker and Sutton, 1968), a P-velocity model (NWPB1) was found for which computed travel times for observed epicentral distances and focal depths were generally in agreement (observed minus computed travel times are usually less than ±4.0 sec) with observed travel times. The model is listed in Table 7 and plotted in Figure 13. The uppermost 25 km of the model is not derived from these data; but is, of necessity, merely a rough estimate for the average P-velocity distribution which might exist under Midway, Wake, and Marcus islands. (Since a great majority of the earthquakes had foci deeper than 25 km, no consideration was given to the P velocity distribution which might exist in the uppermost 25 km of the source locations.) Epicentral distances, focal depths, and observed minus computed travel times for NWPB1 are listed in Table 8.

To obtain some feeling for the uniqueness of this model, travel times were computed for several variations of NWPB1. These models are also listed in Table 7 and plotted in Figure 14. Table 9 is a listing of the travel-time residuals for all of the models tested. The

residuals are grouped in 50 km intervals according to the maximum depth of penetration (vertex) of their respective ray paths. The mean values and the standard deviations of the mean values of these travel time residuals, within the 50 km intervals, are also given in Table 9. Event 24 (previously mentioned as having an anomalously early arrival) and intermediate- and deep-focus earthquakes recorded at short distances (8.97 to 10.39 degrees) were not used in this listing. They will be discussed later. Also, residuals for events having their vertices at depths greater than 400 km are not listed since the theoretical travel times for these events do not differ greatly among the various NWPB models. Of the nine models tested, the residuals of Table 9 suggest that models 1, 3, 6, and 9 are acceptable (means are less than their standard deviations) for the data considered, while models 2, 4, 5, 7, and 8 are not. Models 1, 3, and 6 have low-velocity zones with thicknesses of 75 km terminating at depths of 100, 125, and 150 km, respectively. Model 9, with a velocity of 7.95 km/sec at the top of the mantle, represents the limiting case of models with a thin high velocity cap immediately below the M discontinuity. Models 2, 4, 5, 7, and 8 have low-velocity zones with thicknesses of 50, 25, 50, 75, and 150 km, respectively, terminating at depths of 100, 100, 125, 175, and 250 km, respectively. It is interesting to note that the least acceptable models (7 and 8) have deep low-velocity zones, while the acceptable models have shallower low-velocity zones.

In all of the models tested, intermediate- and deep-focus earthquakes recorded at short distances (8.97 to 10.39 degrees) have large positive travel-time residuals which are essentially the same as those

for Model 1 listed in Table 8. This suggests that if any of the models are close to reality, the hypocenters for these earthquakes are further from the recording stations by as much as 50 km. All of these earthquakes occurred at the northern end of the Mariana Islands (19°.0 to 21°.6 north latitude and 143°.0 to 145°.3 east longitude) and their focal depths range from 165 to 383 km.

For distances of 7°.59 to 20°.34, shear arrivals for events having focal depths less than 165 km have large negative travel time residuals, while shear arrivals for events having focal depths greater than 204 km appear to be normal refracted mantle waves. At greater distances (20°.34 to 39°.10), only the normal refracted mantle shear arrivals are observed. A computer-derived shear velocity distribution was not attempted because of the apparent absence of normal refracted mantle shear phases for shallow focus earthquakes at short distances. Also, the poor quality of the longer period (> 1 sec) shear data prevents drawing any conclusions concerning the attenuation factor "Q" ($Q = -2\pi E dN/dE$, where E is energy and N is the number of cycles) for these periods.

Considering the results of Part II and the data presented here, it now appears certain that the P- and S- phases observed on hydrophones at distances less than 33° represent some sort of high-frequency guided phase. The sharp cut-off at 33° may be due to the fact that earthquakes beyond this distance were located well outside of the Northwestern Pacific Basin (i.e., on the continental side of the circum-Pacific arc), and were therefore unable to transmit a significant amount of energy into the high-frequency waveguide. It is also probable that the depth

of occurrence and extent of the high frequency waveguide for P waves is identical with that for S waves [from Part II, $V_p/V_s = 8.28/4.79 = (2.99)^{1/2}$]. Also, the similarity between travel times of hydrophone high-frequency S waves and those of seismograph high-frequency S waves strongly suggests that both are equivalent.

The apparent velocity for the guided P phase of 8.28±0.03 km/sec (from Part II) agrees well with velocities immediately below the M discontinuity and for the top of the mesosphere in most of the models tested. This value is also close to the average value (8.27 km/sec) obtained from the available marine seismic refraction measurements in this region [Hussong and Odegard, preliminary interpretation of unpublished data, 7.95 km/sec, water depth of 6 km, 27°N and 154°E; Den et al. (1969), 8.6 km/sec, water depth of 6 km, 33°N and 152°E; and Murauchi et al. (1968), 8.11 km/sec, water depth of 5 km, 24°N and 146°E]. In addition, the M discontinuity is generally recognized to be an efficient propagator of high frequencies (Shurbet; 1962, 1964); and the hydrophone data of Part II suggests that the mesosphere underlying the Northwestern Pacific Basin has a high-Q relative to its asthenosphere for frequencies of 3 to 8 Hz. Therefore, from velocity and Q considerations two depth locations appear possible for the high-frequency waveguide: either immediately below the M discontinuity or near the top of the mesosphere. If the layer is placed immediately below the M discontinuity, the high-frequency phases are Pn and Sn phases as suggested by Molnar and Oliver (1969). Both the poor excitation of the guided phases by deeper events and the clear recordings of the guided phases from instruments located on the ocean bottom and on islands favor this latter interpretation.

Considering, further, the combined hydrophone and seismograph data, the following can be noted: (1) the hydrophones are relatively insensitive to 1 to 2 Hz signals and most of the apparent energy of arrivals at teleseismic distances has frequencies in the range of 3 to 8 Hz; (2) the seismographs are relatively insensitive to 3 to 8 Hz signals and most of the apparent energy of arrivals at teleseismic distances has frequencies of less than 3 Hz; (3) low frequencies (< 3 Hz) of the guided P phase are not well transmitted - guided P was observed only on the hydrophones; (4) low frequencies (< 3 Hz) of the guided S phase are somewhat better transmitted - guided S was observed on hydrophones and seismographs; (5) guided phases appear to be strongly excited by sources above 165 km depth and poorly excited by sources below 204 km depth; (6) normal refracted mantle P contains a significant amount of high-frequency energy (> 3 Hz) for distances greater than 33° (observed on hydrophones) and relatively little for shorter distances (not observed on hydrophones except for deep events; based on one deep event, arrival 61 of Part II); and (7) normal refracted mantle S contains relatively little high-frequency energy (> 3 Hz) and was never observed on hydrophone records.

These observations are consistent with an upper mantle structure having an asthenosphere of relatively low Q for frequencies of 3 to 8 Hz compared to that for material above and below. In addition, signals from the high-frequency waveguide (most likely immediately below the M discontinuity) contain little low-frequency energy (< 3 Hz for P), possibly indicating that the waveguide is thin. Differences between P and S signals might be explained by differences in wavelength for a

given frequency. Further, more quantitative, studies concerning the above are in preparation.

Data (Events South of 12° North Latitude)

Coast and Geodetic Survey epicentral data for this region are given in Table 10 and travel times and residuals are given in Table 11. Several short- and long-period seismograms are presented in Figure 15. Throughout the observation range, compressional waves have arrival times which are slightly later than the expected times of arrival of the J-B P phase. Most shear phases are unclear or not apparent. In the few cases that S waves are well recorded, travel times are close to the travel times of the J-B S phase. No significant phases other than the first arrivals are observed. The frequencies of the arrivals are as expected for normal refracted mantle P and S phases.

Discussion (Events South of 12° North Latitude)

The travel-time data suggest that the compressional and shear phases observed are normal refracted mantle arrivals throughout the range of observation. The travel time residuals of the normal refracted mantle P waves suggests lower P-velocities in the mantle than in the J-B model. Since no P wave data were available for epicentral distances of less than 15°.98, any computer-derived P-velocity mantle distribution would be poorly determined in its upper layers. Therefore, no such model is presented. As in Part II, it is found that shear waves are not well recorded for this area; so no attempt was made to derive an S-velocity distribution.

A direct comparison of the seismograph arrivals with the arrivals reported by Carder and Bailey (1958), Jeffreys (1962), and Doyle and

Webb (1963) is not possible. The only P phases of this study recorded at comparable distances were from 2 earthquakes located just south of Guam recorded at Marcus. These 2 phases were recorded at epicentral distances of 15°.98 and 21°.74 with travel time residuals of +5.8 and +5.7 sec, respectively. P phases recorded from the nuclear detonations at Bikini and Eniwetok at similar distances (17°.1, 17°.1, 18°.6, 18°.6, 18°.6, 20°.1, 20°.2, 20°.2, and 20°.4, and 20°.5) were recorded at Guam and Rabaul. The travel time residuals for these phases are from -9 to -2 sec. Since similar travel paths were not involved, it is not yet known what significance should be given to the differences of these data.

Considering the combined hydrophone and seismograph data, the following can be noted: (1) low frequencies (< 3 Hz) of the guided P phases are not well transmitted - guided P phases were observed only on the hydrophones; (2) no guided S phases were observed either on the hydrophones or on the seismographs - however, only one event was recorded at short distance (< 20°); (3) guided P phases appear to be strongly excited by sources above 85 km and poorly excited by sources below 213 km depth; and (4) normal refracted mantle P phases have high-frequency energy for distances greater than 22° and relatively little high-frequency energy for shorter distances, except for two deep-focus events which are recorded on the hydrophones.

These observations, although not nearly as complete, indicate a somewhat similar mantle structure to that found for the area north of 12° north latitude. However, there appear to be some differences between the mantles of the two regions: for the normal refracted mantle P phases recorded in the distance range of 22° to 40°,

travel time residuals are generally slightly negative (13 of the 31 residuals are positive) for the area to the north while travel time residuals are generally slightly positive (only 2 of the 40 residuals are negative) for the area to the south; velocities for the guided P phase north and south of 12° north latitude may be different (8.28 ± 0.03 km/sec with an intercept of +1.4 sec for the area to the north and 8.47 ± 0.48 km/sec with an intercept of +15.0 sec for the area to the south), although this difference is not actually significant due to the large scatter (±0.48 km/sec) of the data for the area to the south; and, a weaker waveguide for shear phases than observed for the area to the north is suggested by the absence of strong guided S phases for the area to the south at distances and focal depths for which strong guided S phases are observed for the area to the north.

IV. FINAL REMARKS

In general, the major conclusions of this study are that: (1) a low-velocity channel for compressional waves is present in the mantle underlying the Northwestern Pacific Basin; (2) this low-velocity zone probably begins very close to the M discontinuity and its Q for frequencies of 3 to 8 Hz is low relative to that for material above and below; (3) a waveguide exists for P and S waves under the Northwestern Pacific Basin and for P waves under the East Caroline Basin-Ontong Java Plateau-Nauru Sea area which propagates 3 to 8 Hz frequencies to great distances; (4) a low Q zone for frequencies of 3 to 8 Hz is also present under the East Caroline Basin-Ontong Java Plateau-Nauru Sea area; and (5) differences are present in the mantles underlying the Northwestern Pacific Basin and the East Caroline Basin-Ontong Java Plateau-Nauru Sea area as indicated by differences in the travel times of P waves recorded at distances beyond 22° and by differences in the attenuation of the guided shear waves for these two regions.

In retrospect, Parts II and III of this dissertation could be viewed as two pieces of a large puzzle which have been successfully fitted together. The data of Part II suggested the existence of the waveguide and provided some quantitative information on its propagation velocities for P and S waves. The data of Part III suggested the existence of a low-velocity zone for P waves and provided some quantitative information on its depth, extent, and velocity. The combined data of Parts II and III further strengthened the waveguide interpretation of the hydrophone arrivals, indicated a zone of low Q for the mantle underlying the Northwestern Pacific Basin and East Caroline

Basin-Ontong Java Plateau-Nauru Sea area, and suggested differences in the mantle under these two regions.

By no means are these "two pieces" of the puzzle considered to be the only pieces to be found and fitted together. The results of this investigation clearly points to the need for obtaining more information on the compressional velocity, shear velocity, and Q distribution for the mantle in the two areas studied. The ultimate objective would be unique compressional velocity, shear velocity, and Q models for the mantle of the Northwestern Pacific Basin and East Caroline Basin-Ontong Java Plateau-Nauru Sea area. Such information would be a significant contribution towards an understanding of the mechanisms by which the sea-floor spreads and all related geological phenomena are produced. The author views this dissertation as a first step towards this objective.

BIBLIOGRAPHY

Caloi, P. (1953). Onde longitudinali e transversali guidate dall' astenosfera Atti accad. nax. Lincei Rend. Classe Sci Fis, Mat. Nat. 8, 352-357.

Carder, D. S. and L. F. Bailey (1958). Seismic wave travel times from nuclear explosions, Bull. Seism. Soc. Am. 48, 377-398.

Den, N., W. J. Ludwig, S. Murauchi, J. I. Ewing, H. Hotta, N. T. Edgar, T. Yoshii, T. Asanuma, K. Hagiwara, T. Sato, and S. Ando (1969). Seismic-refraction measurements in the Northwest Pacific Basin, J. Geophys. Res. 74, 1421-1434.

Doyle, H. A. and J. P. Webb (1963). Travel times to Australian stations from Pacific nuclear explosions in 1958, J. Geophys. Res. 68, 1115-1120.

Gutenburg, Beno (1959). Physics of the Earth's Interior, Academic Press, New York.

Herrin, E. (1968). 1968 seismological tables for P phases, Bull. Seism. Soc. Am. 58, 1193-1241.

Jeffreys, H. (1962). Travel times for Pacific explosions, Geophys. J. Roy. Astron. Soc. 7, 212-219.

Jeffreys, Harold and K. E. Bullen (1958). Seismological Tables, Office of the British Association, Burlington House, W. I. London.

Molnar, Peter and Jack Oliver (1969). Lateral variations of attenuation in the upper mantle and discontinuities in the lithosphere, J. Geophys. Res. 74, 2648-2682.

Murauchi, S., N. Den, S. Asano, H. Hotta, T. Asanuma, K. Ichikawa, T. Sato, W. J. Ludwig, J. I. Ewing, N. T. Edgar, and R. E. Houtz (1968). Crustal structure of the Philippine Sea, J. Geophys. Res. 73, 3143-3171.

Oliver, Jack and Bryan Isacks (1967). Deep earthquake zones, anomalous structures in the upper mantle, and the lithosphere, J. Geophys. Res. 72, 4259-4275.

Press, Frank (1968). Earth models obtained by Monte Carlo inversion, J. Geophys. Res. 73, 5223-5234.

Press, Frank (1969). The suboceanic mantle, Science 165, 174-176.

Raitt, R. W., G. G. Shor, Jr., T. J. G. Francis, and G. B. Morris (1969). Anisotrophy of the Pacific upper mantle, J. Geophys. Res. 74, 3095-3109.

Shurbet, D. H. (1962). High-frequency P and S phases, Bull. Seism. Soc. Am. 52, 597-962.

Shurbet, D. H. (1964). The high-frequency S phase and structure of the upper mantle, J. Geophys. Res. 69, 2065-2070.

Sutton, George H. and Daniel A. Walker (1970). Seismological bulletin, Northwestern Pacific island stations, 1967-1968, Hawaii Institute of Geophysics Data Report No. 15.

Walker, Daniel A. (1965). A study of the northwestern Pacific upper mantle, Bull. Seism. Soc. Am. 55, 925-939.

Walker, Daniel A. and George H. Sutton (1968). The agreement of proposed earth models with observed body-wave travel times, Bull. Seism. Soc. Am. 58, 1059-1069.

Table 1. (hydrophone data)

UNITED STATES COAST AND GEODETIC SURVEY DATA FOR EVENTS NORTH OF 12° NORTH LATITUDE

Event No.	Date	Time	Coordinates	Depth (km)	Mag.
1	27 Jan. 1965	01:44:36.0	18.9°N 176.6°E	33	4.4
2	28 July 1967	05:39:59.0	14.5°N 147.1°E	33	4.3
3	20 April 1965	17:15:19.4	14.8°N 146.9°E	60	5.8
4	23 May 1966	14:22:32.5	13.8°N 146.4°E	39	5.9
5	12 June 1966	07:20:26.0	13.1°N 146.3°E	160	4.2
6	21 Feb. 1967	09:11:55.2	14.1°N 146.4°E	70	5.2
7	5 May 1965	23:23:24.9	14.7°N 146.2°E	56	5.4
8	11 Dec. 1966	20:08:22.3	13.4°N 146.0°E	50	5.6
9	11 Dec. 1966	19:52:09.4	13.4°N 145.8°E	59	5.4
10	20 April 1966	02:32:51.8	18.8°N 146.9°E	23	5.0
11	22 April 1966	13:00:58.8	19.0°N 146.8°E	18	4.6
12	7 May 1965	02:29:03.9	13.9°N 145.4°E	57	4.9
13	27 Oct. 1966	02:27:49.7	14.1°N 145.3°E	125	5.2
14	24 Sept. 1965	23:53:42.7	13.1°N 145.2°E	57	5.5
15	11 Nov. 1965	17:22:26.7	14.0°N 145.0°E	130	5.1
16	11 July 1965	19:09:31.8	13.3°N 144.7°E	57	4.8
17	27 Nov. 1966	13:41:19.0	17.5°N 145.4°E	214	5.5
18	14 April 1966	09:46:56.7	13.5°N 144.5°E	86	4.3
19	14 July 1965	04:37:03.1	13.3°N 144.6°E	52	4.5
20	9 May 1966	00:03:37.5	14.4°N 144.5°E	107	4.8
21	25 Sept. 1966	04:49:36.9	19.2°N 145.7°E	133	5.5
22	7 Nov. 1965	05:42:25.3	14.0°N 144.2°E	41	4.7
23	5 Jan. 1966	18:10:00.9	21.8°N 146.8°E	35	5.5
24	2 Jan. 1965	13:44:18.9	19.1°N 145.4°E	142	6.1
25	2 Jan. 1965	18:10:15.5	19.1°N 145.4°E	145	5.3
26	2 Sept. 1966	09:09:03.0	13.6°N 144.2°E	91	4.9
27	8 Sept. 1965	07:01:33.3	19.2°N 145.3°E	152	5.4
28	10 Feb. 1966	14:21:11.2	20.8°N 146.3°E	46	6.2
29	3 July 1967	03:42:18.2	12.3°N 143.9°E	33	5.0
30	27 Oct. 1966	09:18:15.5	20.2°N 145.6°E	118	5.4
31	22 Jan. 1964	17:58:16.3	20.2°N 147.1°E	39	5.1
32	12 Sept. 1965	03:11:24.1	21.6°N 145.7°E	68	4.8
33	27 Oct. 1966	14:21:04.8	22.2°N 145.9°E	29	6.0
34	29 April 1967	06:24:59.0	19.3°N 146.2°E	114	4.8
35	29 May 1967	02:51:09.4	19.8°N 146.0°E	42	5.5
36	30 Dec. 1965	01:15:21.5	21.6°N 144.5°E	120	5.2
37	7 Jan. 1965	12:54:09.4	19.3°N 145.5°E	120	5.2
38	29 Aug. 1966	08:27:09.0	22.6°N 145.0°E	173	4.7
39	30 March 1965	02:27:07.2	50.6°N 177.9°E	51	$6\frac{1}{4}$–$7\frac{1}{4}$
40	7 Aug. 1966	02:13:05.1	50.6°N 171.3°W	39	6.5
41	29 July 1965	08:29:21.2	50.9°N 171.4°W	22	6.3
42	2 June 1966	03:27:53.3	51.1°N 176.0°E	41	6.0
43	7 Sept. 1963	22:00:57.1	27.5°N 141.5°E	46	4.9
44	10 May 1964	05:39:42.6	29.0°N 141.5°E	62	5.3
45	28 Aug. 1963	15:51:06.3	28.3°N 141.0°E	96	5.1
46	28 Dec. 1965	20:32:25.0	27.8°N 141.8°E	37	5.9
47	1 May 1966	18:30:41.8	30.6°N 140.6°E	114	5.0
48	5 Feb. 1964	11:30:15.7	36.5°N 141.0°E	46	5.4
49	14 Oct. 1963	13:21:45.2	44.8°N 151.0°E	60	5.9
50	15 Nov. 1963	21:05:31.0	44.3°N 149.0°E	50	6.0
51	13 Oct. 1963	05:17:57.1	44.8°N 149.5°E	60	8.0
52	12 Oct. 1963	11:25:57.9	44.8°N 149.0°E	33	$6\frac{1}{4}$–7
53	2 May 1964	16:11:00.2	45.5°N 150.3°E	35	5.7
54	31 May 1964	00:40:36.4	43.5°N 146.8°E	48	6.3
55	10 March 1966	04:26:19.7	32.2°N 137.6°E	382	5.6
56	3 May 1964	01:54:33.5	40.3°N 141.9°E	59	4.8
57	12 Dec. 1963	23:21:36.6	46.3°N 150.5°E	90	5.2
58	10 Jan. 1964	04:50:53.4	42.0°N 142.6°E	33	5.5
59	28 Oct. 1963	12:03:19.8	52.8°N 159.8°E	33	5.7
60	24 Jan. 1964	17:17:45.5	38.7°N 129.4°E	542	5.3
61	1 June 1967	03:06:19.0	53.7°N 165.7°W	60	5.7
62	12 March 1966	16:31:20.6	24.2°N 122.6°E	48	7–8

Table 2. (hydrophone data)

TRAVEL TIMES AND RESIDUALS FOR EVENTS NORTH OF 12° NORTH LATITUDE

Arrival No.	Event No.	Distance (degrees)	Depth (km)	*P* Travel Times			*S* Travel Times		
				J-B (secs)	Observed (secs)	Residual (secs)	J-B (secs)	Observed (secs)	Residual (secs)
1	1	9.4	33	133.2	128.0	−5.2	241.8	226.0	−15.8
2	1	11.4	33	164.2	161.0	−3.2	291.9	273.0	−18.9
3	2	15.0	33	211.2	206.0	−5.2	376.9	361.0	−15.9
4	3	15.3	60	213.3	204.6	−8.7	381.1	360.6	−20.5
5	4	15.6	39	218.7	212.5	−6.2	390.5	370.5	−20.0
6	5	15.6	160	212.3	200.0	−12.3	380.4	355.0	−25.4
7	6	15.8	70	219.4	211.8	−7.6	392.2	369.8	−22.4
8	7	15.9	56	221.8	213.1	−8.7	396.7	376.1	−20.6
9	8	16.1	50	224.7	219.7	−5.0	401.4	382.7	−18.7
10	9	16.2	59	225.2	213.6	−11.6	402.5	374.6	−27.9
11	10	16.4	23	232.5	224.2	−8.3	414.7	392.2	−22.5
12	11	16.6	18	232.5	224.2	−8.3	415.3	392.2	−23.1
13	12	16.6	57	230.6	225.1	−5.5	412.3	392.1	−20.2
14	13	16.7	125	227.8	228.3	+0.5	408.3	398.3	−10.0
15	14	16.9	57	233.9	226.3	−7.6	418.6	399.3	−19.3
16	15	17.2	130	233.6	236.3	+2.7	418.3	412.3	−6.0
17	16	17.2	57	238.1	238.2	+0.1	—	NC	—
18	17	17.3	214	230.0	241.0	+11.0	413.7	415.0	+1.3
19	18	17.4	86	238.9	234.3	−4.6	427.8	411.3	−16.5
20	19	17.5	52	241.7	237.9	−3.8	432.7	416.9	−15.8
21	20	17.5	107	238.8	234.5	−4.3	428.0	409.5	−18.5
22	21	17.6	133	238.4	239.1	+0.7	427.7	420.1	−7.6
23	22	17.8	41	245.7	235.7	−10.0	439.7	405.7	−34.0
24	23	17.9	35	247.6	246.1	−1.5	443.0	429.1	−13.9
25	24	17.9	142	241.1	241.1	0.0	432.5	424.1	−8.4
26	25	17.9	145	241.1	241.5	+0.4	432.5	422.5	−10.0
27	26	17.9	91	244.4	240.0	−4.4	437.8	421.0	−16.8
28	27	18.0	152	242.7	243.7	+1.0	435.9	424.7	−11.2
29	28	18.1	46	250.0	244.8	−5.2	446.9	430.8	−16.1
30	29	18.1	33	250.4	246.8	−3.6	448.3	434.8	−13.5
31	30	18.3	118	247.3	246.5	−0.8	444.1	436.5	−7.6
32	31	18.4	39	253.3	245.7	−7.6	—	NC*	—
33	32	18.6	68	254.8	252.9	−1.9	457.1	441.9	−15.2
34	33	18.8	29	259.9	258.2	−1.7	465.3	453.2	−12.1
35	34	19.1	114	256.6	254.0	−2.6	461.9	451.0	−10.9
36	28	19.2	46	263.2	258.8	−4.4	471.8	453.8	−18.0
37	35	19.5	42	266.5	263.6	−2.9	478.7	463.6	−15.1
38	33	19.6	29	269.0	269.2	+0.2	483.1	470.2	−12.9
39	30	19.8	118	263.4	267.5	+4.1	474.8	473.5	−1.3
40	6	20.6	70	275.4	278.8	+3.4	496.9	480.8	−16.1
41	36	20.8	120	271.5	280.5	+9.0	494.8	491.5	−3.3
42	37	20.9	120	274.7	283.6	+8.9	—	NC	—
43	27	21.1	152	274.6	284.7	+10.1	—	NC	—
44	38	21.6	173	276.8	289.0	+12.2	560.2	512.0	+11.8
45	39	21.9	51	290.2	292.8	+2.6	523.8	510.8	−13.0
46	40	22.7	39	299.2	303.9	+4.7	—	NC	—
47	41	23.1	22	304.2	311.8	+7.6	549.3	561.8	+12.5
48	42	23.7	41	308.7	314.7	+6.0	—	NC	—
49	43	24.1	46	312.0	323.9	+11.9	—	NC	—
50	44	24.4	62	313.6	329.4	+15.8	—	NC	—
51	45	24.6	96	312.8	331.7	+18.9	—	NC	—
52	46	25.2	36	324.1	347.0	+22.9	584.6	605.0	+20.4
53	47	27.6	114	338.5	373.0	+34.5	—	NC	—
54	48	27.6	46	345.5	374.3	+28.8	622.5	654.3	+31.8
55	49	27.7	60	345.2	370.8	+25.6	621.9	643.8	+21.9
56	50	28.2	50	350.4	380.0	+29.6	631.3	658.0	+26.7
57	51	28.3	60	350.3	377.9	+27.6	—	NC	—
58	52	28.4	33	353.4	382.1	+28.7	—	NC	—
59	53	28.5	35	354.2	381.8	+27.6	638.0	665.8	+27.8
60	54	28.6	48	354.1	383.6	+29.5	634.6	665.6	+31.0

Table 2. (continued)

Arrival No.	Event No.	Distance (degrees)	Depth (km)	*P* Travel Times			*S* Travel Times		
				J-B (secs)	Observed (secs)	Residual (secs)	J-B (secs)	Observed (secs)	Residual (secs)
61	55	29.0	382	328.8	328.3	−0.5	—	NA†	—
62	56	29.1	59	357.4	391.5	+34.1	—	NC	—
63	57	29.1	90	354.6	390.0	+35.4	—	NC	—
64	58	29.6	33	364.4	398.6	+34.2	—	NC	—
65	59	32.9	33	393.1	446.2	+53.1	707.3	773.2	+65.9
66	33	33.1	29	395.9	460.2	+64.3	—	NC	—
67	40	35.8	39	417.5	417.9	+0.4	—	NA	—
68	6	36.6	70	421.0	419.8	−1.2	—	NA	—
69	60	36.9	542	384.1	380.5	−3.6	—	NA	—
70	61	39.7	60	448.1	445.0	−3.1	—	NA	—
71	62	39.8	48	449.0	454.4	+5.4	—	NA	—

* NC, Not clear. † NA, Not apparent.

Table 3. (hydrophone data)

UNITED STATES COAST AND GEODETIC SURVEY DATA FOR EVENTS SOUTH OF 12° NORTH LATITUDE

Event No.	Date	Time	Coordinates	Depth (km)	Mag.
1	4 March 1967	22:41:14.5	7.8°N 146.2°E	20	5.1
2	6 July 1965	18:36:47.4	4.5°S 155.1°E	510	6.4
3	28 Aug. 1966	10:03:03.0	4.6°S 155.2°E	509	5.6
4	22 June 1967	19:08:33.5	1.3°S 149.8°E	34	5.0
5	7 Sept. 1966	15:55:11.5	5.1°S 154.7°E	77	5.5
6	3 Sept. 1965	21:38:53.8	5.3°S 153.7°E	54	5.9
7	30 July 1967	13:35:14.4	5.3°S 153.6°E	50	5.2
8	23 Oct. 1966	09:15:48.0	6.5°S 155.2°E	34	5.0
9	8 June 1966	03:42:13.7	7.7°S 158.9°E	55	5.1
10	29 July 1967	14:19:04.0	7.0°S 155.8°E	85	4.6
11	10 April 1967	15:02:42.2	7.3°S 155.8°E	29	5.6
12	28 Oct. 1966	01:41:19.1	9.6°S 159.8°E	32	5.5
13	17 July 1965	07:20:30.7	9.7°S 159.8°E	24	6.4
14	17 May 1967	12:56:55.4	9.7°S 159.8°E	32	5.1
15	14 May 1967	12:24:03.9	10.5°S 161.4°E	37	5.4
16	7 June 1966	13:59:36.0	11.3°N 139.6°E	50	6.5
17	13 June 1967	15:39:29.7	5.6°S 148.1°E	213	5.4
18	5 Oct. 1966	14:00:27.3	10.7°S 162.4°E	82	4.8
19	13 June 1966	18:08:38.4	12.2°S 167.1°E	259	6.2
20	2 Feb. 1967	18:18:17.4	4.3°S 153.7°E	247	5.0
21	13 June 1967	15:39:29.7	5.6°S 148.1°E	213	5.4
22	30 July 1967	17:24:43.1	17.8°S 178.8°W	564	5.1
23	21 July 1966	18:30:14.9	17.8°S 178.6°W	591	5.6
24	8 Sept. 1966	21:15:52.8	2.4°N 128.4°E	96	6.9
25	17 March 1966	15:50:33.1	21.1°S 179.2°W	639	6.2

Table 4. (hydrophone data)

TRAVEL TIMES AND RESIDUALS FOR EVENTS SOUTH OF 12° NORTH LATITUDE

Arrival No.	Event No.	Distance (degrees)	Depth (km)	*P* Travel Times		
				J-B (secs)	Observed (secs)	Residual (secs)
1	1	16.4	20	230.7	228.5	−2.2
2	2	17.6	510	215.8	217.6	+1.8
3	3	17.6	509	216.1	218.0	+1.9
4	4	17.9	34	247.9	246.5	−1.4
5	5	18.3	77	249.9	251.5	+1.6
6	6	18.9	54	258.7	267.2	+8.5
7	7	19.0	50	260.5	266.6	+6.1
8	8	19.4	34	265.9	274.0	+8.1
9	9	19.6	55	266.5	268.3	+1.8
10	10	19.6	85	265.0	273.0	+8.0
11	11	20.4	29	277.6	290.8	+13.2
12	12	21.1	32	283.9	295.9	+12.0
13	13	21.2	24	284.5	292.3	+7.8
14	14	21.4	32	286.9	298.6	+11.7
15	15	21.9	37	291.9	299.1	+7.2
16	16	22.2	50	293.5	296.0	+2.5
17	17	22.2	213	279.4	280.3	+0.9
18	18	22.2	82	290.8	309.7	+18.9
19	19	24.2	259	294.9	294.6	−0.3
20	20	26.0	247	312.5	312.6	+0.1
21	3	26.3	509	296.2	294.0	−2.2
22	16	27.2	50	341.7	340.0	−1.7
23	21	30.2	213	352.8	354.3	+1.5
24	22	34.5	564	363.1	363.9	+0.8
25	23	34.9	591	365.0	367.1	+2.1
26	24	34.9	96	404.0	405.2	+1.2
27	25	37.4	639	383.0	384.9	+1.9
28	22	39.6	564	404.8	404.9	+0.1
29	23	39.6	591	404.1	404.1	0.0

Table 5. (seismograph data)

United States Coast and Geodetic Survey
Data for Events North of 12°North Latitude

Arrival No.	Date	Time	Coordinates	Depth (km)	Mag.
1	5 Apr. 1967	02:47:55.4	20.0°N 147.2°E	50	5.7
2	5 Apr. 1967	02:34:11.1	20.0°N 147.1°E	50	5.9
3	4 Oct. 1968	19:11:18.6	19.5°N 147.1°E	41	5.0
4	6 Feb. 1969	07:33:00.5	21.8°N 145.7°E	56	5.2
5	17 Oct. 1968	06:53:16.7	18.7°N 146.4°E	70	4.9
6	16 Jan. 1969	17:06:39.8	20.8°N 144.9°E	165	4.5
7	14 Oct. 1968	07:27:32.5	22.5°N 144.3°E	31	4.9
8	17 Jun. 1969	19:26:28.9	19.0°N 145.5°E	206	5.8
9	22 Jun. 1969	18:40:09.5	19.0°N 145.5°E	134	4.4
10	18 Oct. 1968	02:47:25.5	18.9°N 145.3°E	225	4.8
11	11 May 1969	12:10:04.9	17.8°N 145.9°E	135	4.9
12	1 Feb. 1969	03:35:14.9	17.8°N 145.9°E	115	5.1
13	7 Jul. 1969	04:43:15.4	16.5°N 147.3°E	38	5.7
14	27 Mar. 1969	08:23:13.6	19.5°N 144.6°E	383	4.6
15	21 Nov. 1968	14:32:13.0	18.8°N 145.0°E	229	5.2
16	12 Jul. 1969	05:55:40.1	17.6°N 145.7°E	204	4.5
17	27 Aug. 1969	19:23:10.6	28.7°N 143.8°E	20	5.4
18	11 Nov. 1968	06:49:13.9	24.6°N 142.7°E	22	5.2
19	28 Jul. 1969	15:37:56.2	24.1°N 142.7°E	N	5.2
20	15 Aug. 1969	08:41:54.9	21.6°N 142.0°E	319	6.1
21	27 Mar. 1969	20:47:24.5	16.2°N 146.1°E	66	5.2
22	30 Jul. 1969	04:18:44.5	28.5°N 142.6°E	N	5.1
23	4 Jun. 1969	19:38:12.6	28.0°N 142.4°E	N	4.8
24	7 Oct. 1968	19:20:20.3	26.3°N 140.6°E	516	6.1
25	15 Sept. 1969	16:59:37.6	29.4°N 140.9°E	103	4.7
26	29 Oct. 1968	06:26:58.2	31.2°N 141.7°E	40	5.1
27	29 Oct. 1968	06:45:15.4	31.2°N 141.7°E	33	5.1
28	29 Oct. 1968	04:06:04.1	31.2°N 141.6°E	17	5.7
29	9 Mar. 1969	14:06:18.9	31.2°N 141.6°E	33	5.2
30	6 Sept. 1969	16:17:15.5	30.0°N 140.6°E	89	5.3
31	15 May 1967	02:27:36.0	32.5°N 141.4°E	40	5.4
32	6 Aug. 1969	08:40:39.2	32.5°N 140.6°E	67	4.9
33	13 Sept. 1969	11:19:03.9	33.8°N 141.6°E	35	5.0
34	28 Oct. 1968	14:40:41.4	33.4°N 140.8°E	61	5.5
35	18 Aug. 1969	09:29:48.8	34.2°N 140.7°E	46	4.8
36	8 Aug. 1969	04:55:10.0	36.4°N 141.4°E	41	5.4
37	31 Oct. 1969	07:09:13.4	37.1°N 142.0°E	40	5.0
38	23 Jul. 1969	13:14:35.1	37.3°N 141.5°E	53	5.2
39	16 Aug. 1968	10:39:16.8	38.5°N 143.3°E	22	5.6
40	16 Mar. 1969	15:54:17.2	38.5°N 142.7°E	40	5.4
41	14 Oct. 1968	09:11:27.5	38.2°N 142.1°E	69	5.0
42	1 Jul. 1968	10:45:11.9	36.0°N 139.3°E	67	5.9
43	13 Jun. 1968	03:48 12.8	39.1°N 143.2°E	28	4.7
44	4 Nov. 1969	08:50:46.9	33.8°N 137.1°E	347	5.4
45	5 Aug. 1969	18:34:33.3	37.9°N 140.6°E	130	5.0
46	5 Jul. 1968	11:38:12.6	38.5°N 142.0°E	43	5.9
47	9 Apr. 1969	17:57:34.8	36.8°N 139.6°E	116	5.5
48	13 Jun. 1968	11:56:23.4	39.2°N 143.0°E	33	5.3
49	20 Jun. 1969	06:41:06.2	38.6°N 141.8°E	86	5.4
50	12 Jun. 1968	21:57:41.3	39.3°N 142.8°E	36	5.7
51	13 Jun. 1968	21:10:35.4	39.4°N 142.9°E	39	5.5

Table 5. (continued)

Arrival No.	Date	Time	Coordinates	Depth (km)	Mag.
52	4 Dec. 1969	08:50:21.6	40.7°N 144.7°E	70	5.7
53	11 Nov. 1968	14:41:15.9	40.1°N 143.0°E	35	5.5
54	18 Oct. 1969	01:13:59.7	39.3°N 141.4°E	107	5.3
55	24 Nov. 1968	21:20:59.9	40.3°N 142.3°E	51	5.9
56	24 May 1968	14:06:24.2	40.9°N 143.0°E	38	5.6
57	17 Jun. 1968	11:53:00.4	41.0°N 143.0°E	48	5.7
58	27 Oct. 1966	14:21:04.8	22.2°N 145.9°E	29	6.0
59	15 Aug. 1969	04:32:00.4	43.0°N 147.9°E	N	5.6
60	14 Aug. 1969	14:19:01.6	43.1°N 147.5°E	N	6.1
61	16 Aug. 1969	17:13:44.0	43.2°N 147.7°E	53	5.4
62	12 Aug. 1969	05:53:28.2	43.7°N 148.5°E	N	5.4
63	11 Aug. 1969	21:27:39.4	43.5°N 147.4°E	28	7.1
64	30 Aug. 1969	08:28:06.5	43.6°N 147.8°E	N	5.4
65	30 Aug. 1969	07:11:33.5	43.7°N 147.8°E	N	5.4
66	12 Aug. 1969	11:21:21.6	43.9°N 148.7°E	29	5.4
67	7 Oct. 1968	20:49:01.3	42.0°N 142.4°E	32	5.7
68	6 Sept. 1969	07:43:29.8	43.7°N 147.3°E	N	5.5
69	21 Sept. 1968	13:05:58.2	42.2°N 142.6°E	33	5.9
70	13 Aug. 1969	08:31:32.2	44.0°N 147.7°E	N	5.6
71	8 Mar. 1969	10:20:09.3	41.3°N 139.6°E	169	5.7
72	21 Apr. 1969	07:19:27.5	32.2°N 131.9°E	41	6.1
73	17 Sept. 1969	18:40:45.8	31.1°N 131.3°E	8	6.2
74	17 Aug. 1969	11:54:54.9	42.7°N 141.4°E	130	5.6
75	3 Aug. 1969	07:48:11.4	45.4°N 151.8°E	13	5.3
76	31 Mar. 1969	19:25:27.2	38.3°N 134.6°E	417	5.9
77	12 Jul. 1969	13:09:36.9	46.5°N 153.3°E	12	5.3
78	4 Sept. 1969	03:03:52.0	46.6°N 153.5°E	N	5.4
79	19 Jan. 1969	07:02:04.0	45.0°N 143.2°E	204	6.4
80	31 Oct. 1969	11:33:04.8	51.3°N 179.0 W	49	6.0-6.3
81	3 Aug. 1968	04:54:32.7	25.6°N 128.5°E	19	6.4
82	12 Nov. 1968	00:44:12.8	27.5°N 128.4°E	48	5.8
83	2 Oct. 1969	22:06:09.0	51.4°N 179.2°E	1	6.5
84	21 Oct. 1969	20:53:47.5	51.3°N 178.9°W	48	5.4-5.9
85	19 Mar. 1969	13:59:22.7	28.8°N 128.2°E	136	5.8
86	20 Aug. 1969	07:50:05.5	47.9°N 153.6°E	73	5.8
87	27 May 1967	17:22:58.7	51.9°N 176.1°E	34	5.8
88	1 Dec. 1967	13:57:02.4	49.5°N 154.4°E	136	5.9
89	31 Jul. 1969	11:23:01.2	53.0°N 179.1°W	37	5.3
90	13 Jun. 1969	08:48:29.5	49.4°N 155.5°E	64	5.9
91	16 Aug. 1968	19:39:16.8	38.5°N 143.3°E	22	5.6
92	16 Jul. 1969	08:16:53.3	52.2°N 154.0°E	69	5.8
93	17 Jan. 1967	11:59:31.5	38.3°N 142.1°E	44	5.9
94	23 Sept. 1968	05:03:50.0	40.3°N 143.5°E	30	4.8
95	1 Jul. 1967	23:10:07.2	54.4°N 158.0°W	33	6.2
96	21 Sept. 1968	13:05:58.2	42.2°N 142.6°E	33	5.9
97	22 Nov. 1969	23:09:37.2	57.8°N 163.5°E	N	6.3-7.3
98	18 Jul. 1969	05:24:48.0	38.3°N 119.4°E	N	6.2
99	2 Oct. 1969	22:06:00.0	51.4°N 179.2°E	1	6.5
100	11 Aug. 1968	12:37:28.1	52.1°N 179.9°E	159	5.5
101	11 Aug. 1968	12:37:28.1	52.1°N 179.9°E	159	5.5
102	22 Nov. 1969	23:09:37.2	57.8°N 163.5°E	N	6.3-7.3
103	17 Jan. 1967	11:59:31.5	38.3°N 142.1°E	44	5.9
104	7 Aug. 1966	02:13:05.1	50.6°N 171.3°W	39	6.5
105	28 Jan. 1967	13:52:58.3	52.4°N 160.5°W	47	6.7
106	9 Sept. 1969	05:15:37.7	35.7°N 137.0°E	29	5.5-6.0

Table 6. (seismograph data)

Travel Times and Residuals for Events North of 12° North Latitude

Arrival No.	Distance (degrees)	Depth (km)	Mag.	Station	P Travel Times			S Travel Times		
					J-B (secs)	Observed (secs)	Residual (secs)	J-B (secs)	Observed (secs)	Residual (secs)
1	7.59	50	5.7	MCS	110.9	106.6*	-4.3*	--	NC‡*	--
2	7.67	50	5.9	MCS	112.3	104.3*	-8.0*	--	NC*	--
3	7.80	41	5.0	MCS	113.8	109.9	-3.9	201.8	190.9	-10.9
4	7.93	56	5.2	MCS	115.2	112.5	-2.7	203.7	194.5	-9.2
5	8.81	70	4.9	MCS	126.9	123.3	-3.6	225.6	214.5	-11.1
6	8.97	165	4.5	MCS	127.1	NA†* 127.5	-- +0.4	226.5	218.0* 213.3	-8.5* -13.2
7	9.00	31	4.9	MCS	130.8	128.5	-2.3	231.9	218.1	-13.8
8	9.30	206	5.8	MCS	131.3	131.6* 132.1	+0.3* +0.8	234.1	NA* 233.9	-- -0.2
9	9.30	134	4.4	MCS	132.4	130.4* 129.9	-2.0* -2.5	235.8	221.0* 224.4	-14.8* -11.4
10	9.54	225	4.8	MCS	133.8	135.5	+1.7	238.6	243.5	+4.9
11	9.76	135	4.9	MCS	138.0	138.6	+0.6	246.0	238.6	-7.4
12	9.76	115	5.1	MCS	--	NC	--	246.7	236.1	-10.6
13	9.76	38	5.7	MCS	141.0	141.2* 140.8	+0.2* -0.2	250.5*	241.6* 239.7	-8.9* -10.8
14	9.79	383	4.6	MCS	136.5	139.7	+3.2	--	NA	--
15	9.83	229	5.2	MCS	137.5	138.3	+0.8	245.3	256.5	+11.2
16	10.03	204	4.5	MCS	--	NC	--	250.4	NA* 253.4	+3.0
17	10.25	20	5.4	MCS	149.2	143.7* 143.4	-5.5* -5.8	264.8	246.2* 246.3	-18.6* -18.5
18	10.28	22	5.2	MCS	--	NC	--	265.8	246.2	-19.6
19	10.29	N	5.2	MCS	--	NA* NA	-- --	263.7	NA* 247.2	-- -16.5
20	10.39	319	6.1	MCS	143.7	143.7* 144.1	0.0* +0.4	257.2	256.1* NA	-1.1* --
21	10.74	66	5.2	MCS	--	NC	--	272.7	264.7	-8.0
22	11.14	N	5.1	MCS	160.0	NA* 151.2	-- -8.8	--	NA* NC	-- --
23	11.50	N	4.8	MCS	164.7	157.9	-6.8	292.9	280.4	-12.5
24	12.31	516	6.1	MCS	162.5	142.2* 141.2	-20.3* -21.3	--	NA* NC	-- --

Table 6. (continued)

Arrival No.	Distance (degrees)	Depth (km)	Mag.	Station	P Travel Times			S Travel Times		
					J-B (secs)	Observed (secs)	Residual (secs)	J-B (secs)	Observed (secs)	Residual (secs)
25	12.85	103	4.7	MCS	--	NA* NC	--	320.9	NA* 308.0	-- -12.9
26	13.02	40	5.1	MCS	184.9	177.8	-7.1	--	NC	--
27	13.02	33	5.1	MCS	185.3	178.6	-6.7	--	NC	--
28	13.09	17	5.7	MCS	188.0	181.4	-6.6	334.5	314.2	-20.3
29	13.10	33	5.2	MCS	186.3	179.5	-6.8	--	NC	--
30	13.32	89	5.3	MCS	186.6	NA* 180.4	-- -6.2	--	NA* NC	-- --
31	13.74	40	5.4	MCS	193.9	188.0*	-5.9*	--	NC*	--
32	14.50	67	4.9	MCS	203.0	NA* 197.5	-- -5.5	--	NA* NC	-- --
33	14.58	35	5.0	MCS	205.6	NA* 198.9	-- -6.7	366.9	NA* 346.1	-- -20.8
34	14.86	61	5.5	MCS	208.0	203.1* 202.6	-4.9* -5.4	371.4	NA* 351.4	-- -20.0
35	15.42	46	4.8	MCS	215.9	211.2	-4.7	385.5	363.7	-21.8
36	16.44	41	5.4	MCS	229.1	220.0	-9.1	--	NC	--
37	16.63	40	5.0	MCS	--	NC	--	414.3	390.8	-23.5
38	17.05	53	5.2	MCS	236.2	NA* 229.4	-- -6.8	422.6	NA* 402.6	-- -20.0
39	17.09	22	5.6	MCS	239.2	232.6	-6.6	--	NC	--
40	17.38	40	5.4	MCS	241.0	235.3	-5.7	431.2	412.8	-18.4
41	17.41	69	5.0	MCS	239.6	235.0	-4.6	--	NC	--
42	17.42	67	5.9	MCS	239.9	234.5*	-5.4*	--	NC*	--
43	17.62	28	4.7	MCS	245.1	239.2*	-5.9*	--	NC*	--
44	17.68	347	5.4	MCS	225.2	225.7	+0.5	--	NA	--
45	17.69	130	5.0	MCS	--	NC	--	429.5	416.6	-12.9
46	17.70	43	5.9	MCS	244.8	235.4*	-9.4*	438.2	416.4*	-21.8*
47	17.77	116	5.5	MCS	241.2	238.7	-2.5	432.7	419.4	-13.3
48	17.79	33	5.3	MCS	246.6	240.1*	-6.5*	--	NC*	--
49	17.90	86	5.4	MCS	244.5	241.2* 241.5	-3.3* -3.0	438.0	422.5* 423.0	-15.5* -15.0

Table 6. (continued)

Arrival No.	Distance (degrees)	Depth (km)	Mag.	Station	P Travel Times			S Travel Times		
					J-B (secs)	Observed (secs)	Residual (secs)	J-B (secs)	Observed (secs)	Residual (secs)
50	17.96	36	5.7	MCS	248.5	241.8*	-6.7*	--	NC*	--
51	18.00	29	5.5	MCS	249.7	246.3*	-3.4*	--	NC*	--
52	18.42	70	5.7	MCS	255.9	NA* 251.0	-- -4.9	457.8	NA* 443.9	-- -13.9
53	18.54	35	5.5	MCS	255.7	251.6	-4.1	--	NC	--
54	18.63	107	5.3	MCS	251.5	246.9	-4.6	452.1	437.3	-14.8
55	19.00	51	5.9	MCS	260.1	255.6	-4.5	--	NC	--
56	19.21	38	5.6	MCS	263.4	256.8*	-6.6*	--	NC*	--
57	19.30	48	5.7	MCS	263.6	257.4*	-6.2*	--	NC*	--
58	19.62	29	6.0	WKE	--	NC	--	482.9	473.1	-9.8
59	19.65	N	5.6	MCS	268.6	269.3* NC	+0.7* --	482.8	NA* 470.2	-- -12.6
60	19.83	N	6.1	MCS	270.6	269.0* 269.5	-1.6* -1.1	486.8	472.4* 465.7	-14.4* -21.1
61	19.89	53	5.4	MCS	--	NC	--	485.2	473.5	-11.7
62	20.20	N	5.4	MCS	--	NC	--	494.5	485.5	-9.0
63	20.23	28	7.1	MCS	--	NC	--	496.1	485.1	-11.0
64	20.24	N	5.4	MCS	275.0	268.9*	-6.1*	--	NC*	--
65	20.34	N	5.4	MCS	276.0	271.2* NA	-4.8* --	--	NC* NA	-- --
66	20.36	29	5.4	MCS	277.0	276.8* NC	-0.2* --	498.4	491.0* 479.6	-7.4* -18.8
67	20.38	32	5.7	MCS	276.5	272.7*	-3.8*	--	NC*	--
68	20.44	N	5.5	MCS	277.1	276.2* NC	-0.9* --	499.2	NA* 487.1	-- -12.1
69	20.48	33	5.9	MCS	277.5	273.8* 274.3	-3.7* -3.2	499.9	NC* 485.8	-- -14.1
70	20.65	N	5.6	MCS	279.2	277.9* NC	-1.3* --	503.1	489.3* 507.4* 487.8	-13.8* +4.3* -15.3
71	21.04	169	5.7	MCS	271.7	270.7	-1.0	--	NC	--
72	21.07	41	6.1	MCS	282.9	284.7* 282.3	+1.8* -0.6	--	NC* NA	-- --

Table 6. (continued)

Arrival No.	Distance (degrees)	Depth (km)	Mag.	Station	P Travel Times			S Travel Times		
					J-B (secs)	Observed (secs)	Residual (secs)	J-B (secs)	Observed (secs)	Residual (secs)
73	21.27	8	6.2	MCS	289.0	285.8* 286.4	-3.2* -2.6	520.6	525.2* NA	+4.6* --
74	21.39	130	5.6	MCS	278.3	277.4* 277.7	-0.9* -0.6	502.7	509.0* NC	+6.3* --
75	21.47	13	5.3	MCS	290.3	NA* 290.9	-- +0.6	--	NA* NA	-- --
76	21.81	417	5.9	MCS	261.0	265.3* 264.8	+4.3* +3.8	--	NA* NA	-- --
77	22.50	12	5.3	MCS	300.8	NA* 301.6	-- +0.8	--	NA* NA	-- --
78	22.60	11	5.4	MCS	298.8	295.3* 294.5	-3.5* -4.3	539.6	546.0* NA	+6.4* --
79	22.75	204	6.4	MCS	285.4	285.8* 285.6	+0.4* +0.2	515.5	513.7* NA	-1.8* --
80	23.12	49	6.0-6.3	MDW	302.5	302.8* 302.8	+0.3* +0.3	546.3	554.2* NA	+7.9* --
81	23.13	19	6.4	MCS	306.0	307.3* 307.8	+1.3* +1.8	552.3	556.3* NA	+4.0* --
82	23.24	48	5.8	MCS	303.7	304.7	+1.0	--	NA	--
83	23.33	48	5.4-5.9	MDW	304.6	302.1	-2.5	--	NA	--
84	23.33	1	6.5	MDW	310.5	309.6	-0.9	--	NA	--
85	23.53	136	5.8	MCS	298.6	299.1* 299.3	+0.5* +0.7	--	NA* NA	--
86	23.90	73	5.8	MCS	307.8	306.5* 307.7	-1.3* -0.1	--	NC* NA	--
87	24.17	34	5.8	MDW	314.4	314.2	-0.2	--	NA	--
88	25.16	136	5.9	MCS	314.6	311.9*	-2.7*	--	NC*	--
89	25.36	37	5.3	MDW	325.2	321.2	-4.0	--	NA	--
90	25.40	64	5.9	MCS	323.3	323.5	+0.2	--	NA	--
91	27.86	22	5.6	WKE	350.2	353.1*	+2.9*	630.7	636.9*	+6.2*
92	28.46	69	5.8	MCS	350.5	348.2* 348.7	-2.3* -1.8	--	NA* NA	-- --
93	28.51	44	5.9	WKE	353.8	353.2	-0.6	--	NA	--
94	28.86	30	4.8	WKE	358.0	356.2	-1.8	--	NA	--
95	29.73	33	6.2	MDW	365.0	364.5	-0.5	--	NA	--

Table 6. (continued)

Arrival No.	Distance (degrees)	Depth (km)	Mag.	Station	P Travel Times			S Travel Times		
					J-B (secs)	Observed (secs)	Residual (secs)	J-B (secs)	Observed (secs)	Residual (secs)
96	30.60	33	5.9	WKE	373.0	372.3*	-0.7*	671.6	667.3*	-4.3*
97	32.47	N	6.3-6.7	MDW	389.5	389.0	-0.5	--	NA	--
98	32.60	N	6.2	MCS	390.6	394.8* 392.8	+4.2* +2.2	--	NC* NA	-- --
99	33.54	1	6.5	MCS	403.3	399.0* 399.0	-4.3* -4.3	--	NC* NA	-- --
100	34.36	159	5.5	WKE	393.5	393.9	+0.4	--	NA	--
101	34.39	159	5.5	MCS	393.7	393.9	+0.2	--	NA	--
102	34.48	N	6.3-7.3	MCS	406.8	404.0*	-2.8*	732.1	738.8*	+6.7*
103	35.34	44	5.9	MDW	411.6	410.9	-0.7	--	NA	--
104	35.80	39	6.5	WKE	417.5	417.4	-0.1	--	NA	--
105	37.91	47	6.7	WKE	434.5	432.2	-2.3	--	NA	--
106	39.10	29	5.5-6.0	MDW	446.3	451.1	+4.8	--	NA	--

‡ NC, Not clear.

† NA, Not apparent.

*, Recorded on the LPZ (no asterisk means that the arrival was recorded on the SPZ). The absence of times for either an SPZ or LPZ arrival means that no such data was available.

Table 7.

P Velocity Distribution for Northwestern Pacific Basin (NWPB) Models

Depth (km)	Velocity (km/sec)								
	NWPB Model Number								
	1	2	3	4	5	6	7	8	9
2	5.00*								
12	6.30*								
25	8.25	8.25	8.25	8.25	8.25	8.25	8.25	8.25	7.95
50	7.95	8.25	8.25	8.25	8.25	8.25	8.25	8.25	7.95
75	7.95	7.95	7.95	8.25	8.25	8.25	8.25	8.25	7.90
100	7.90	7.95	7.95	7.95	7.95	7.95	8.25	8.25	8.10
125	8.25	8.25	7.90	8.25	7.95	7.95	7.95	7.95	8.25
150	8.35	8.35	8.35	8.35	8.35	7.90	7.95	7.95	8.35
175	8.35	8.35	8.35	8.35	8.35	8.45	7.95	7.95	8.35
225	8.35	8.35	8.35	8.35	8.35	8.45	8.35	7.95	8.35
250	8.45	8.45	8.45	8.45	8.45	8.45	8.45	7.95	8.45
300	8.50*								
350	8.70*								
400	8.85*								
450	9.00*								
500	9.35*								
550	9.50*								
600	9.95*								
650	10.30*								
700	10.50*								
750	10.80*								
800	10.95*								
850	11.10*								
900	11.15*								
950	11.20*								
1000	11.35*								

* The same velocity value was used at this depth in models 2 through 9.

Table 8.

Travel Time Residuals for NWPB1 Model

Distance (degrees)	Depth (km)	Residual (secs)	Distance (degrees)	Depth (km)	Residual (secs)	Distance (degrees)	Depth (km)	Residual (secs)
7.59	50	-0.3	17.38	40	+0.1	22.50	12	+3.4
7.67	50	-3.7	17.41	69	+0.7	22.60	33	-3.9
7.80	41	-0.5	17.42	67	+0.0	22.75	204	0.0
7.93	56	+1.3	17.62	28	+0.3	23.12	49	+0.3
8.81	70	+0.9	17.68	347	-0.9	23.13	19	+2.0
8.97	165	+5.0*	17.70	43	-3.9	23.24	48	+0.9
9.00	31	+2.2	17.77	116	+1.9	23.33	48	-2.6
9.30	206	+4.6*	17.79	33	-0.8	23.33	1	-1.5
9.30	134	NA†	17.90	86	+1.3	23.53	136	+0.6
9.54	225	+5.2*	17.96	36	-1.1	23.90	73	-1.0
9.76	135	NA	18.00	29	+2.5	24.17	34	+0.6
9.76	38	+4.7	18.42	70	+3.6	25.16	136	-2.1
9.79	383	+6.0*	18.54	35	+1.1	25.36	37	-3.4
9.83	229	+4.2	18.63	107	-1.2	25.40	64	+1.1
10.25	20	+0.3	19.00	51	-0.2	27.86	22	+4.3
10.39	319	+3.3*	19.21	38	-2.4	28.46	69	-1.7
11.14	33	-3.1	19.30	48	-2.3	28.51	44	+0.5
11.50	33	-1.1	19.65	33	+4.4	28.86	30	-1.0
12.31	516	-21.8	19.83	33	+1.9	29.73	33	-0.2
13.02	40	-0.7	20.24	33	-3.2	30.60	33	0.0
13.02	33	-0.2	20.34	33	-2.1	32.47	33	+0.3
13.09	17	+1.1	20.36	29	+3.0	32.60	33	+3.0
13.10	33	-0.3	20.38	32	-1.1	33.54	1	-2.4
13.32	89	+0.1	20.44	33	+1.7	34.36	159	+0.6
13.74	40	+0.1	20.48	33	-1.2	34.39	159	+0.4
14.50	67	+0.9	20.65	33	+0.9	34.48	33	-2.2
14.58	35	-0.1	21.04	169	-1.2	35.14	44	0.0
14.86	61	+1.1	21.07	41	+0.8	35.80	39	+0.3
15.42	46	+1.7	21.27	8	-0.4	37.91	47	-2.3
16.44	41	-4.0	21.39	130	-1.0	39.10	29	+4.7
17.05	53	-1.0	21.47	13	+2.2			
17.09	22	-0.5	21.81	417	-3.3			

*, p arrivals. † NA, for the given epicentral distance and focal depth no P or p arrivals would be observed in this model.

Table 9.

Travel Time Residuals for NWPB Models*

Depth (km)	Travel Time Residuals (secs) NWPB Model Number 1	2	3	4	5
100	-0.3 3.7 0.5 3.1 1.3 0.7 0.2 0.3 0.1 +1.3 0.9 2.2 4.7 0.3 1.1 0.1 0.1 0.9 +1.1 1.7	-0.1 3.4 2.3 0.3 2.3 +0.2 2.0 1.6 2.8 5.5 1.2 0.6 2.0 0.5 +0.6 0.8 1.4 0.6 1.6 2.3 1.2 0.0	-1.5 4.8 1.1 0.3 3.3 1.3 1.1 0.4 0.6 -0.4 0.2 0.4 +0.6 1.8 0.1 1.0 0.4 0.6 1.3 4.4	-1.4 1.5 +0.8 0.4 4.1 2.4 1.9 3.7 6.3 2.0 0.6 +0.8 1.4 2.9 1.3 1.0 1.6 2.0 2.5 +3.1 0.3 2.1 1.5 2.0	-2.4 0.4 0.1 2.4 +1.3 1.1 2.7 5.4 1.1 0.5 1.9 0.4 0.1 +0.7 1.0 0.5 1.3 2.2 1.2
	0.22 ± 0.39†	0.75 ± 0.39	-0.26 ± 0.42	1.73 ± 0.32	0.85 ± 0.39
150	-1.8 3.9 0.8 1.1 0.2 +0.1 0.7 0.0 0.3 1.3 2.5 3.6 1.1	-0.5 3.2 0.4 +0.7 1.2 0.5 1.2 0.0 1.7 3.3 4.1 0.3	-3.3 1.5 0.3 0.5 4.2 1.0 1.4 +0.2 0.2 0.2 0.7 2.3 3.1	-2.4 +1.6 1.0 2.1 4.6	-0.6 3.3 0.1 0.5 +0.6 0.8 0.1 1.1 1.2 3.2 3.7
	0.20 ± 0.50	0.74 ± 0.54	-0.42 ± 0.55	1.38 ± 1.12	0.56 ± 0.57
200	-4.8 0.5 +4.2	+1.4 1.4	-0.6 +4.2 0.6	-1.3 +2.2 2.0	+1.3
	-0.10 ± 2.37	1.40 ± 0.00	1.40 ± 1.44	0.97 ± 1.13	1.30
250	+1.9	-1.8 1.9 +4.9 2.4	-1.7 2.5 2.7	-1.2 +0.8 5.5 3.0	-1.3 1.9 2.0 +1.8 0.1 4.9
	1.90	0.90 ± 1.67	-2.30 ± 0.30	2.03 ± 1.44	0.27 ± 1.10
300	-1.2 2.4 2.3 3.2 2.1 +4.4 1.9 3.0	-0.9 2.7 1.6 +3.6	-2.2 3.3 +1.4 4.3 1.8 3.0	-0.6 2.1 1.1 +4.1	-2.7 1.6 +2.4 3.6
	-0.24 ± 1.02	-0.40 ± 1.38	0.83 ± 1.21	0.08 ± 1.37	0.43 ± 1.52
350					
400					

Table 9. (continued)

Depth (km)	Travel Time Residuals (secs) — EHPB Model Number 6	7	8	9
		+4.4		+1.3
		4.40		1.30
100				-2.8 -0.5 +1.2 +1.3 0.1 2.3 3.4 0.0 0.3 4.9 2.9 0.3 0.9 1.2 0.5 1.1 0.1 0.1 0.8 0.5
				0.03 ± 0.41
150	-2.2 -0.4 +0.8 +2.2 3.5 0.5 3.8 1.7 1.9 0.4 0.9 0.0 0.6 0.1 0.7 3.3 0.4 2.6 1.0 4.2 1.0 0.5 1.9 2.0 4.7 3.2 1.0 0.0 2.7 0.4 0.7 0.3 0.9 1.0 1.1 1.1	-1.7 -4.7 2.5 1.1 3.2 0.3 3.2 2.6 2.4 0.9 2.6 1.9		-0.8 +2.0 +0.1 3.7 0.3 2.1 0.9 0.6 0.2 0.9 0.5 1.4 2.7 3.9 1.3
	-0.06 ± 0.35	-2.43 ± 0.42		0.35 ± 0.48
200		-3.1 -1.1 +0.8 2.6 5.3 1.8 2.5 1.5 2.5 0.6 3.7 2.7 1.4 1.0 1.7		
		-2.05 ± 0.39		
250	-1.9 +0.1 2.0 4.9 2.4	-1.1 +2.4 3.4	-11.0 -6.4 8.9 5.2 8.1 4.2 7.6 8.4 6.2 6.2 7.7 4.8 6.9 5.0 7.2 8.0 5.5	+4.2
	0.70 ± 1.32	-1.03 ± 1.70	-6.90 ± 0.42	4.20
300	-2.8 +3.4 1.7	-0.2 +0.5 2.3 3.1 3.6 0.6 2.6 2.6	-3.9 -2.7 4.6 4.9 4.3 3.5 8.3 3.5 2.1 5.5 2.8 5.4 1.8 0.1	-1.2 +1.5 2.2 4.5 3.0 2.1 1.9 3.2
	-0.37 ± 1.91	-0.24 ± 0.86	-3.96 ± 0.54	0.37 ± 0.99
350			-1.0 +1.4 6.0 0.3 4.9	
			-2.04 ± 1.45	
400				

*The sign of the residual in any column is equal to the sign of the first entry in that column.

**All residuals appearing above the indicated depth have vertices at shallower depths, and all residuals appearing below the indicated depth have vertices at the indicated depth or at greater depths.

†These values represent the mean($\bar{X}$) and the standard deviation of the mean ($S_{\bar{X}}$) as given by: $\bar{X} = (\sum_{i=1}^{N} X_i) / N$ and $S_{\bar{X}} = [\sum_{i=1}^{N} (X_i - \bar{X})^2 / N(N-1)]^{1/2}$

Table 10. (seismograph data)

United States Coast and Geodetic Survey
Data for Events South of 12° North Latitude

Arrival No.	Date	Time	Coordinates	Depth (km)	Mag.
1	8 Jan. 1969	21:55:48.1	11.8°N 143.1°E	N	5.4
2	27 Jan. 1969	13:15:24.4	8.8°N 137.7°E	5	5.5
3	20 Aug. 1968	11:16:59.3	5.6°N 146.9°E	33	5.6
4	16 Apr. 1969	01:22:47.5	3.5°S 151.0°E	39	5.7
5	31 May 1969	23:56:21.6	4.9°S 154.2°E	403	5.5
6	23 Oct. 1968	21:04:41.3	3.3°S 143.3°E	12	6.1
7	20 Mar. 1969	16:18:56.4	8.7°N 127.3°E	N	6.1
8	18 Aug. 1968	18:38:30.6	10.1°S 159.9°E	538	6.2
9	16 Sept. 1968	13:55:36.1	6.1°S 148.7°E	59	5.8
10	28 Nov. 1968	16:30:32.1	6.8°S 156.2°E	169	5.7
11	16 Sept. 1968	13:55:36.1	6.1°S 148.7°E	59	5.8
12	4 Aug. 1968	11:41:24.8	6.6°N 126.8°E	107	5.7
13	24 Oct. 1968	15:51:18.5	5.9°N 127.0°E	70	5.4
14	31 Jan. 1969	00:44:13.3	4.2°N 128.1°E	N	5.7
15	5 Mar. 1969	13:52:04.9	4.0°N 128.2°E	48	5.7
16	27 Mar. 1969	12:41:35.9	4.8°N 127.5°E	32	6.1
17	3 Feb. 1969	21:41:41.9	4.9°N 127.4°E	N	6.1
18	30 Jan. 1969	10:29:40.4	4.8°N 127.4°E	70	5.9
19	20 Feb. 1969	10:30:22.1	3.5°N 128.4°E	77	6.0
20	20 Feb. 1969	09:55:33.8	3.5°N 128.2°E	33	5.7
21	5 Jan. 1969	13:26:39.9	8.0°S 158.9°E	47	6.4
22	8 Sept. 1968	15:12:23.8	3.7°S 143.0°E	29	6.0
23	4 Nov. 1968	09:07:38.5	14.2°S 172.0°E	585	5.8
24	18 Aug. 1968	18:38:30.6	10.1°S 159.9°E	538	6.2
25	29 Oct. 1968	17:00:40.4	1.8°N 126.4°E	33	5.5
26	24 Jul. 1969	05:03:26.7	1.6°N 126.5°E	41	5.4
27	10 Aug. 1968	05:51:47.5	1.5°N 126.2°E	33	6.2
28	11 Aug. 1968	20:00:43.4	1.6°N 126.1°E	33	5.9
29	10 Aug. 1968	02:07:04.3	1.4°N 126.2°E	33	6.3
30	31 Oct. 1968	09:06:36.4	1.2°N 126.3°E	33	6.1
31	25 Jan. 1969	05:19:17.1	0.8°N 126.1°E	24	5.9
32	6 Jan. 1969	15:39:00.9	10.5°S 164.5°E	32	6.2
33	30 Jan. 1969	18:36:37.3	4.0°N 123.0°E	521	5.3
34	27 May 1969	09:27:03.8	0.2°S 125.0°E	N	5.3
35	24 Feb. 1969	00:08:45.6	6.2°S 131.0°E	38	5.8
36	15 Mar. 1969	11:44:42.3	2.8°S 126.5°E	N	5.6
37	29 Jul. 1968	23:52:15.0	0.2°S 133.4°E	12	6.1
38	4 May 1969	17:18:38.8	0.0°N 123.3°E	165	5.5
39	28 Oct. 1968	23:32:28.7	12.5°S 166.5°E	60	5.9
40	27 Sept. 1968	03:58:55.1	6.8°S 129.1°E	127	6.1
41	19 Aug. 1968	15:42:29.7	15.9°S 174.0°W	151	5.3

Table 11. (seismograph data)

Travel Times and Residuals for Events South of 12° North Latitude

Arrival No.	Distance (degrees)	Depth (km)	Mag.	Station	P Travel Times			S Travel Times		
					J-B (secs)	Observed (secs)	Residual (secs)	J-B (secs)	Observed (secs)	Residual (secs)
1	15.98	N	5.4	MCS	223.8	229.6	+5.8	--	NA†	--
2	21.74	5	5.5	MCS	294.2	299.9	+5.7	--	NA	--
3	23.61	33	5.6	WKE	308.7	311.2*	+2.5*	557.5	555.2*	-2.3*
4	27.56	39	5.7	MCS	345.4	347.8	+2.4	--	NA	--
5	28.81	403	5.5	MCS	324.8	327.8	+3.0	--	NA	--
6	29.11	12	6.1	MCS	362.7	368.2*	+5.5*	--	NC‡*	--
7	29.72	N	6.1	MCS	365.2	366.7	+1.5	--	NA	--
8	30.04	538	6.2	WKE	326.8	327.9* 327.9	+1.1* +1.1	--	NC*	--
9	30.44	59	5.8	MCS	369.1	371.9	+2.8	--	NA	--
10	30.78	169	5.7	MCS	361.8	365.3	+3.5	--	NA	--
11	30.84	59	5.8	WKE	372.7	372.7* 371.4	+0.0* -1.3	--	NC*	--
12	31.33	107	5.7	MCS	372.3	375.2	+2.9	--	NC*	--
13	31.60	70	5.4	MCS	378.2	380.5	+2.3	--	NA	--
14	31.83	N	5.7	MCS	383.9	389.0	+5.1	--	NA	--
15	31.89	48	5.7	MCS	383.0	385.1	+2.1	--	NA	--
16	31.90	32	6.1	MCS	384.7	388.0	+3.3	--	NA	--
17	31.91	N	6.1	MCS	384.6	387.6	+3.0	--	NA	--
18	31.98	70	5.9	MCS	381.5	382.7	+1.2	--	NA	--
19	32.07	77	6.0	MCS	381.7	383.7* 384.2	+2.0* +2.5	--	NC*	--
20	32.22	33	5.7	MCS	387.3	393.0	+5.7	--	NA	--
21	32.25	47	6.4	MCS	386.2	390.9* 391.1	+4.7* +4.9	695.1	697.9*	+2.8*
22	32.60	29	6.0	WKE	391.2	391.8*	+0.6*	--	NC*	--
23	33.80	585	5.8	WKE	356.0	356.5*	+0.5*	641.1	637.5*	-3.6*

Table 11. (continued)

Arrival No.	Distance (degrees)	Depth (km)	Mag.	Station	P Travel Times			S Travel Times		
					J-B (secs)	Observed (secs)	Residual (secs)	J-B (secs)	Observed (secs)	Residual (secs)
24	34.48	538	6.2	MCS	364.3	367.4* 367.6	+3.1* +3.3	--	NC*	--
25	34.69	33	5.5	MCS	408.6	410.1	+1.5	--	NA	--
26	34.75	41	5.4	MCS	408.4	409.6	+1.2	--	NA	--
27	35.04	33	6.2	MCS	411.6	415.0	+3.4	--	NA	--
28	35.05	33	5.9	MCS	411.7	411.1	-0.6	--	NA	--
29	35.11	33	6.3	MCS	412.2	NC* 413.6	 +1.4	--	NC*	--
30	35.17	33	6.1	MCS	412.7	413.6	+0.9	--	NA	--
31	35.59	24	5.9	MCS	417.6	418.9	+1.3	--	NA	--
32	35.88	32	6.2	MCS	419.0	NC* 422.5	 +3.5	--	NC*	--
33	35.92	521	5.3	MCS	377.3	380.7	+3.4	--	NA	--
34	36.96	N	5.3	MCS	427.8	431.6	+3.8	--	NA	--
35	37.48	38	5.8	MCS	431.7	436.2	+4.5	--	NA	--
36	37.72	N	5.6	MCS	434.2	437.7	+3.5	--	NA	--
37	37.86	12	6.1	WKE	438.6	442.3*	+3.7*	789.4	793.0*	+3.6
38	38.08	165	5.5	MCS	424.3	428.1	+3.8	--	NA	--
39	38.37	60	5.9	MCS	436.9	440.3	+3.4	--	NA	--
40	39.08	127	6.1	MCS	436.2	439.9	+3.7	--	NA	--
41	39.88	151	5.3	WKE	440.4	441.3* 441.3	+0.9* +0.9	--	NA*	--

‡, †, and * - See Table 2.

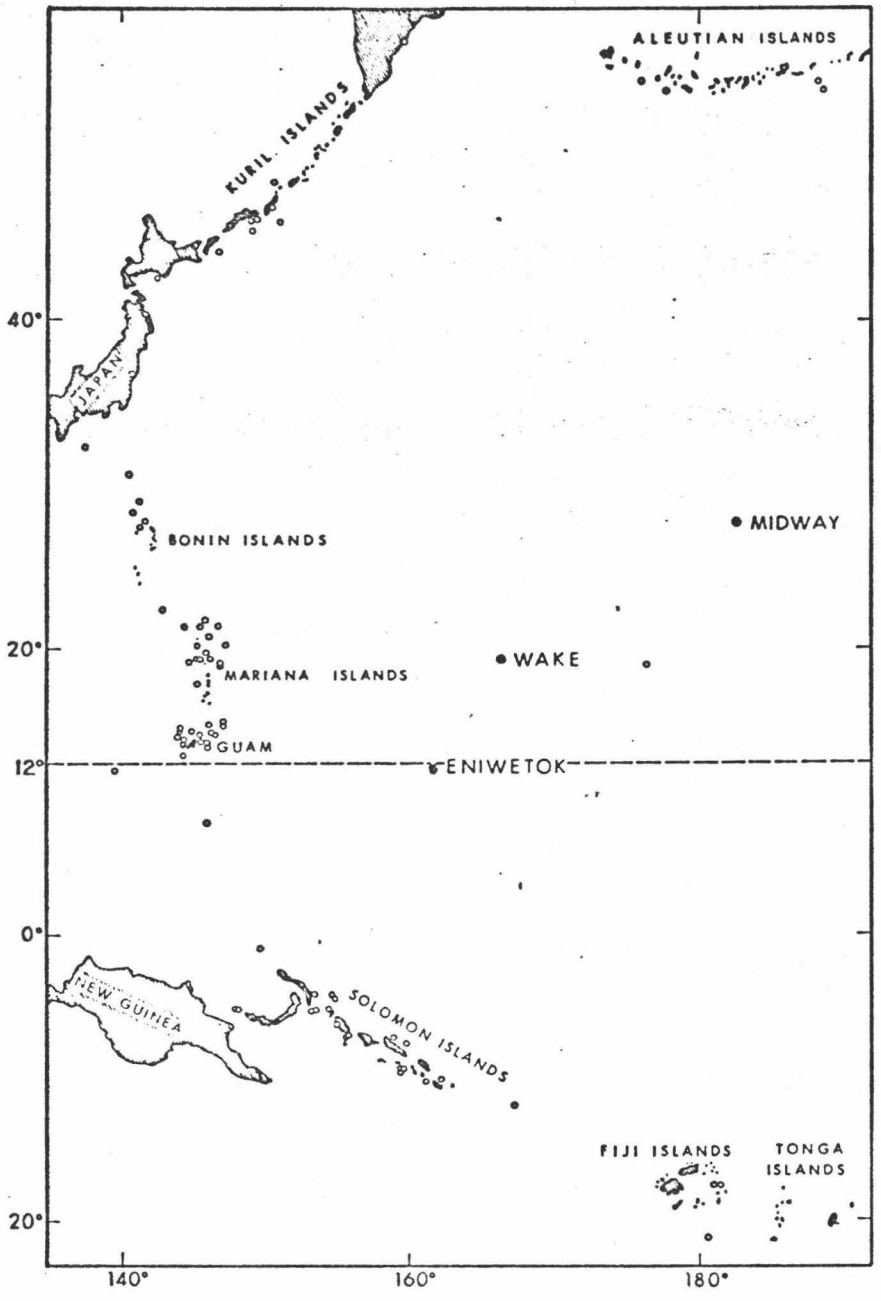

Fig. 1. Epicenter map for hydrophone data.

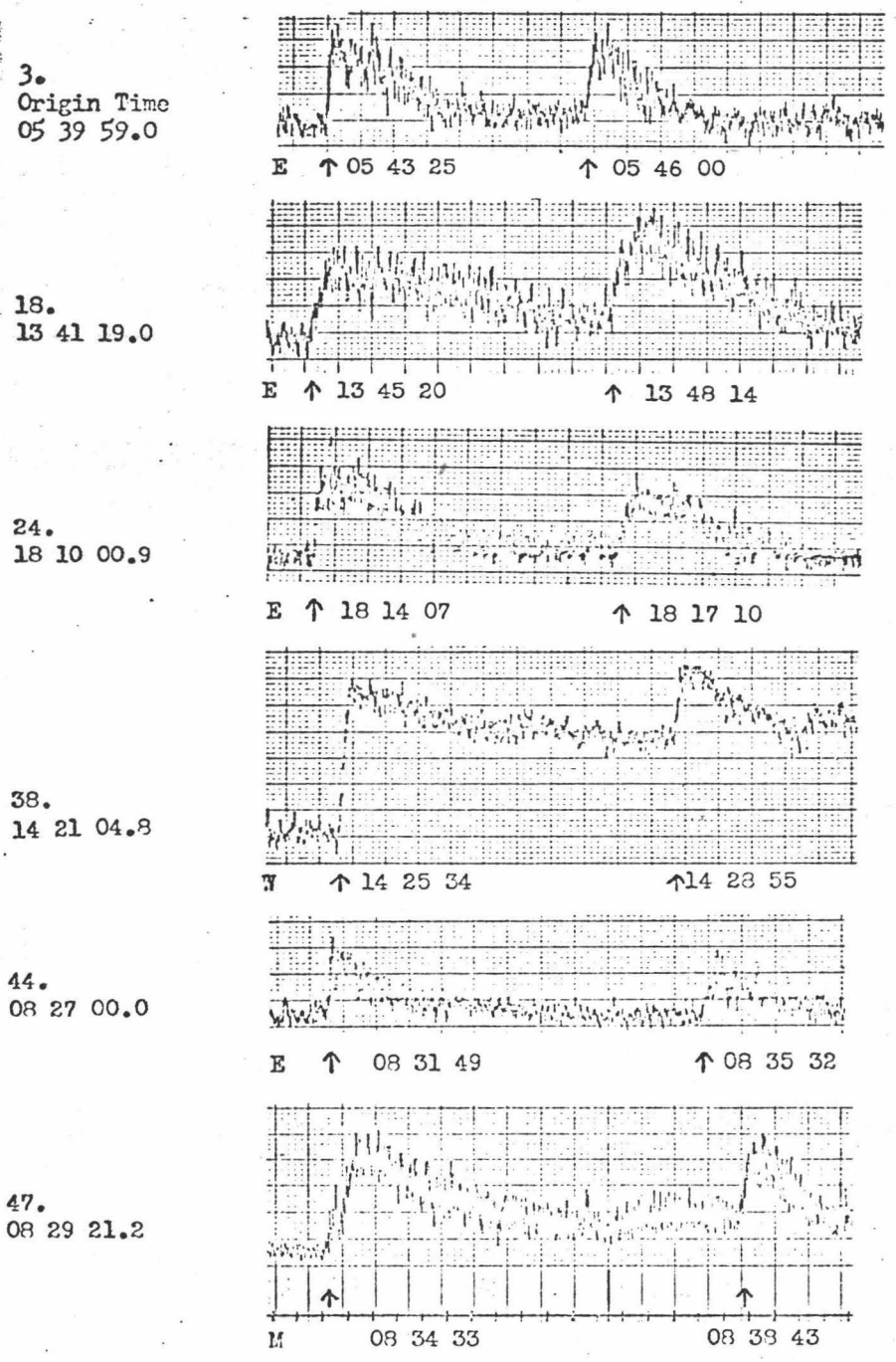

Fig. 2. Observed hydrophone arrivals from events north of 12° north latitude (W - Wake, M - Midway, and E - Eniwetok; a time scale is shown below arrival 47; the interval between tick marks is 15 sec).

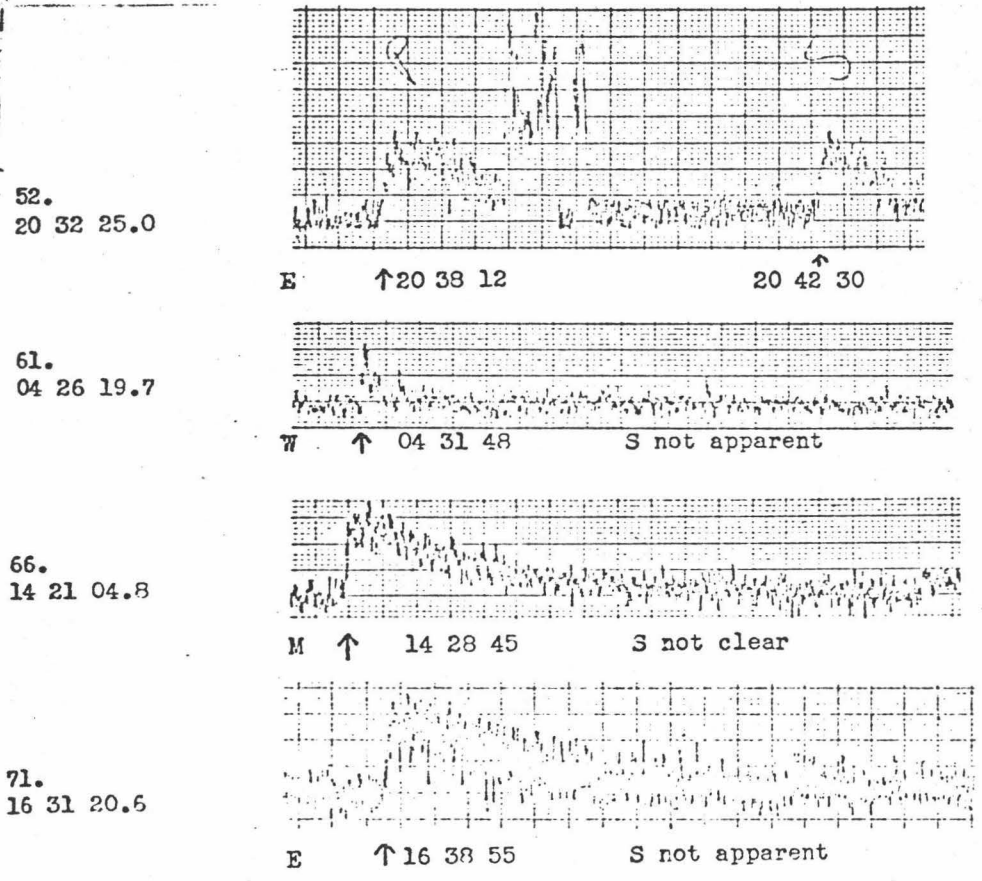

Fig. 2. (continued)

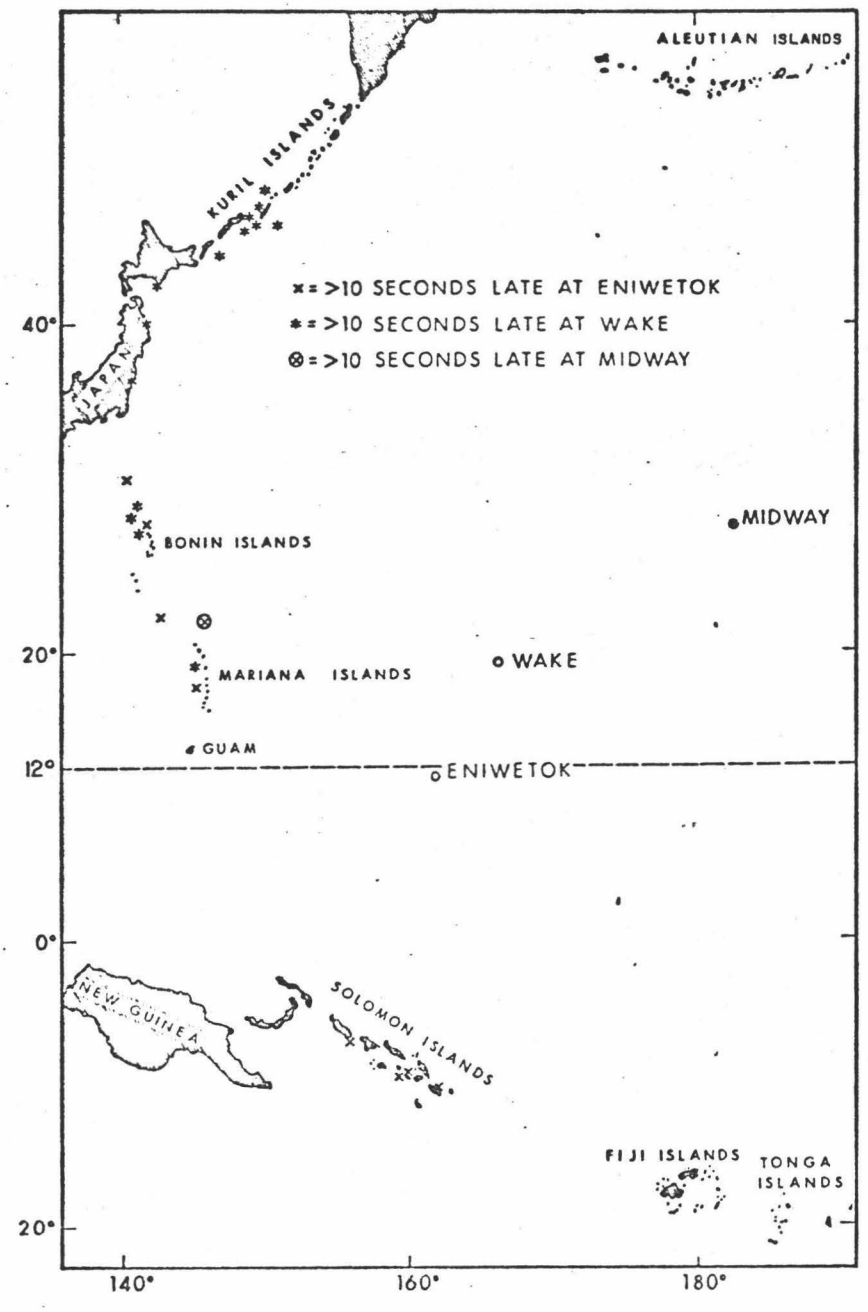

Fig. 3. Epicenter map for events having residuals greater than 10 sec (hydrophone data).

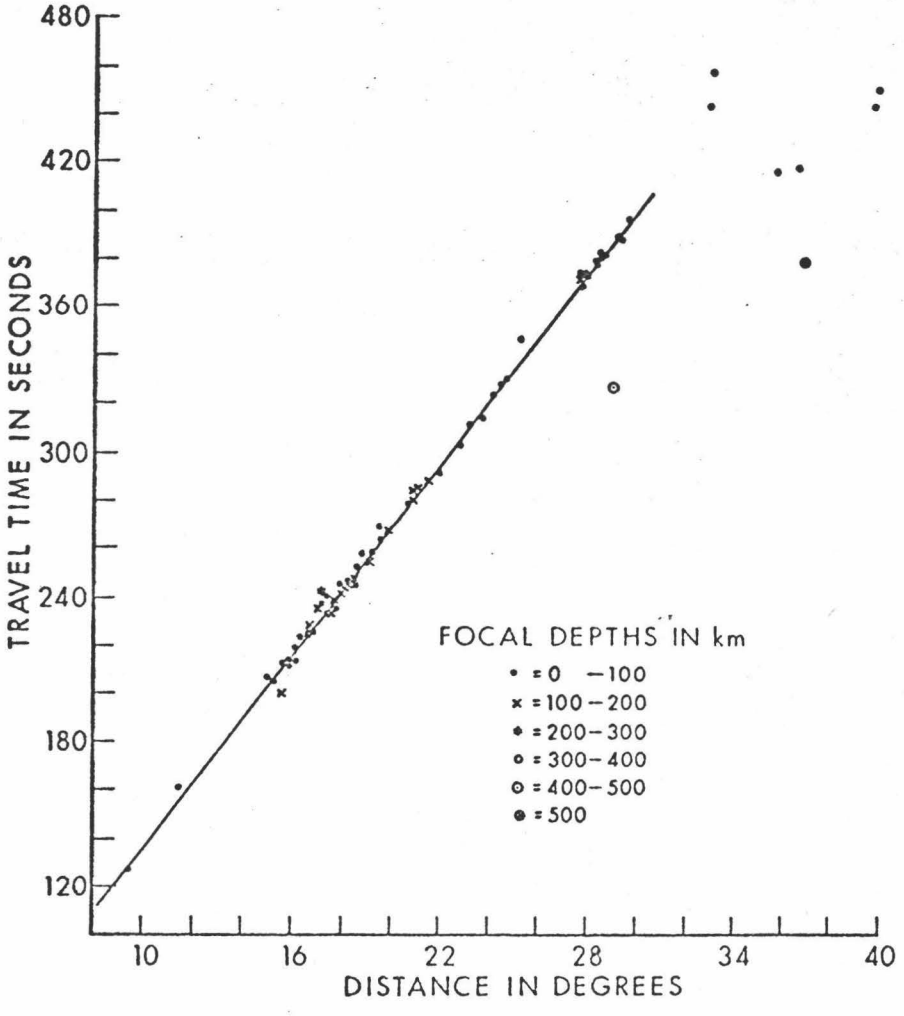

Fig. 4. Travel-time curve for compressional arrivals from events north of 12° north latitude (hydrophone data).

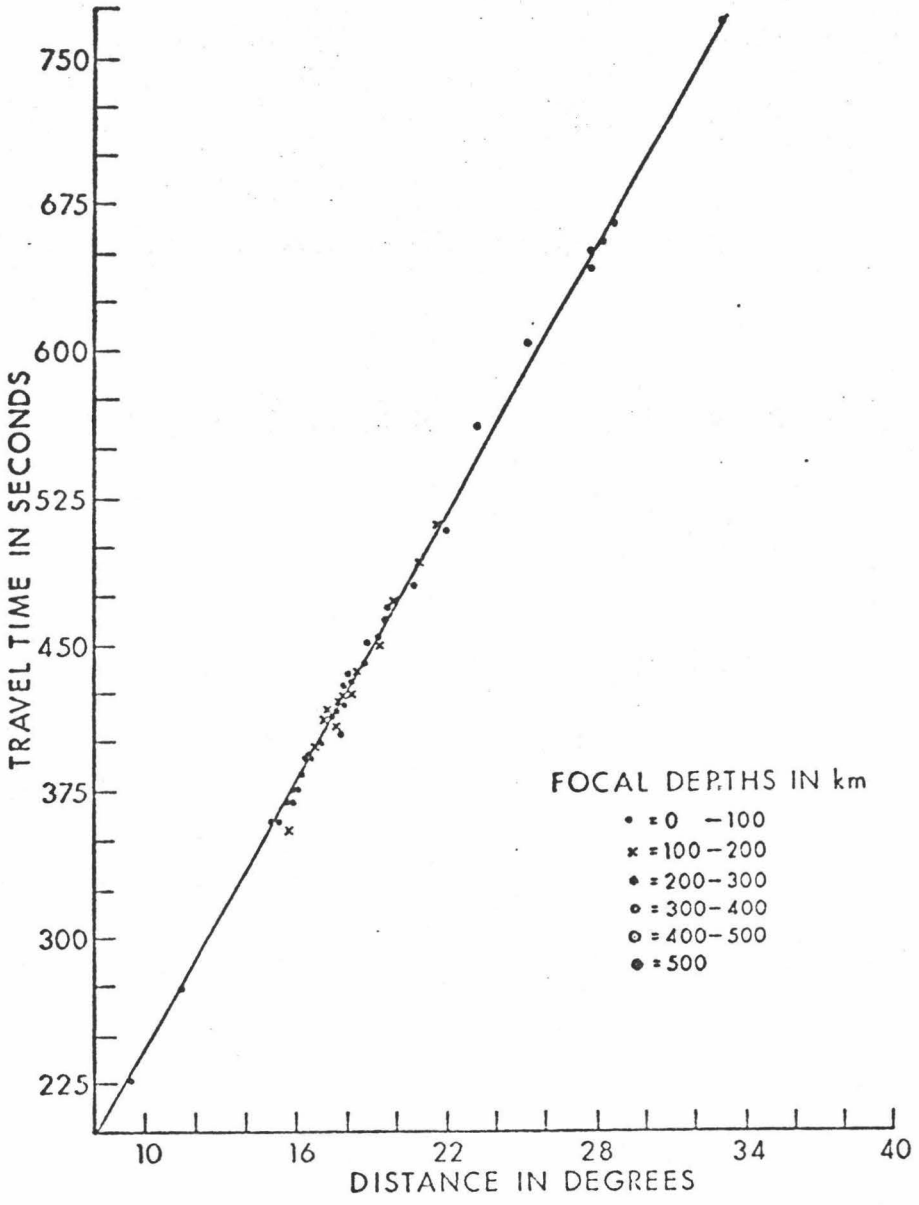

Fig. 5. Travel-time curve for shear arrivals from events north of 12° north latitude (hydrophone data).

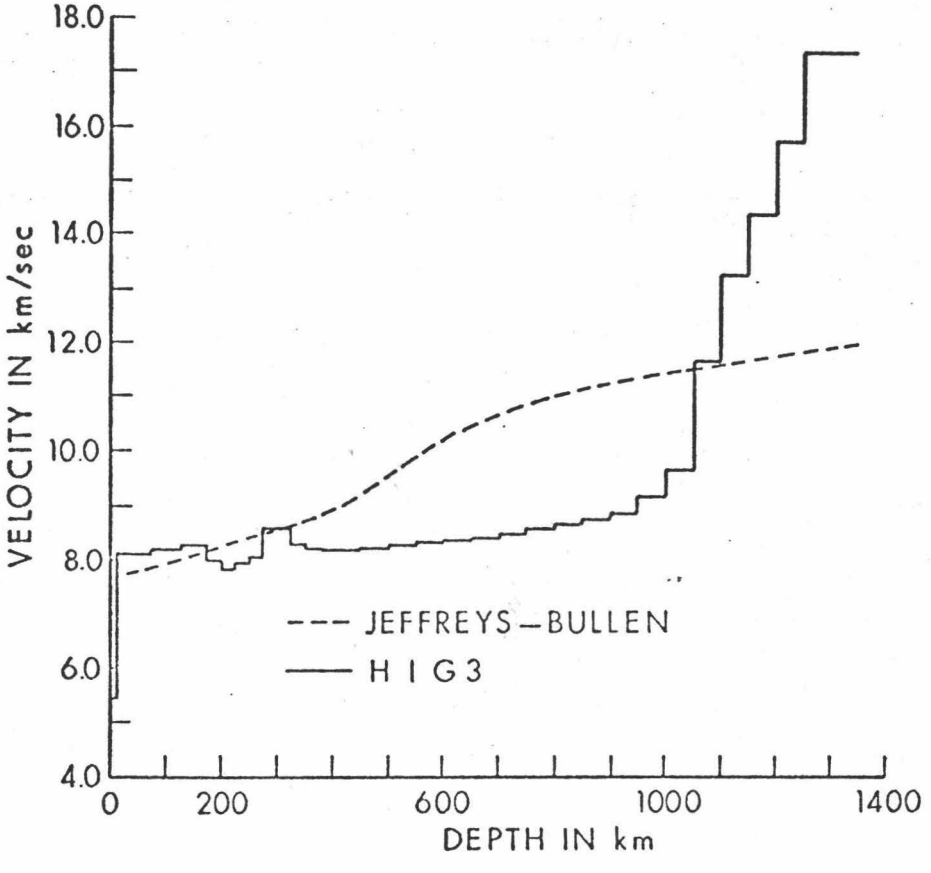

Fig. 6. HIG 3 model for compressional waves north of 12° north latitude (hydrophone data only).

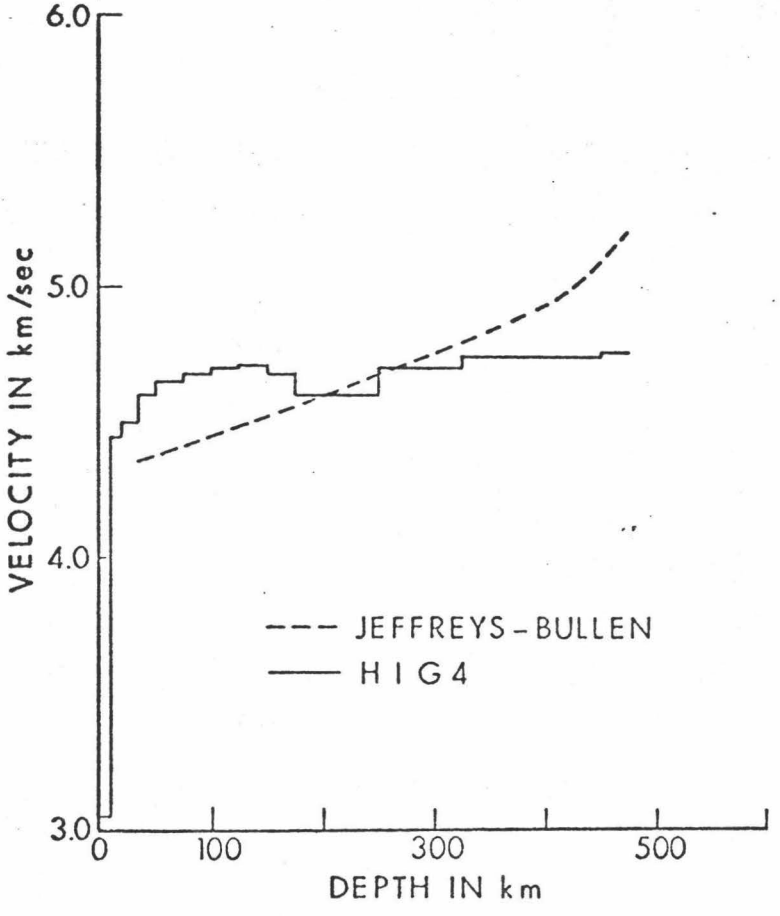

Fig. 7. HIG 4 model for shear waves north of 12° north latitude (hydrophone data only).

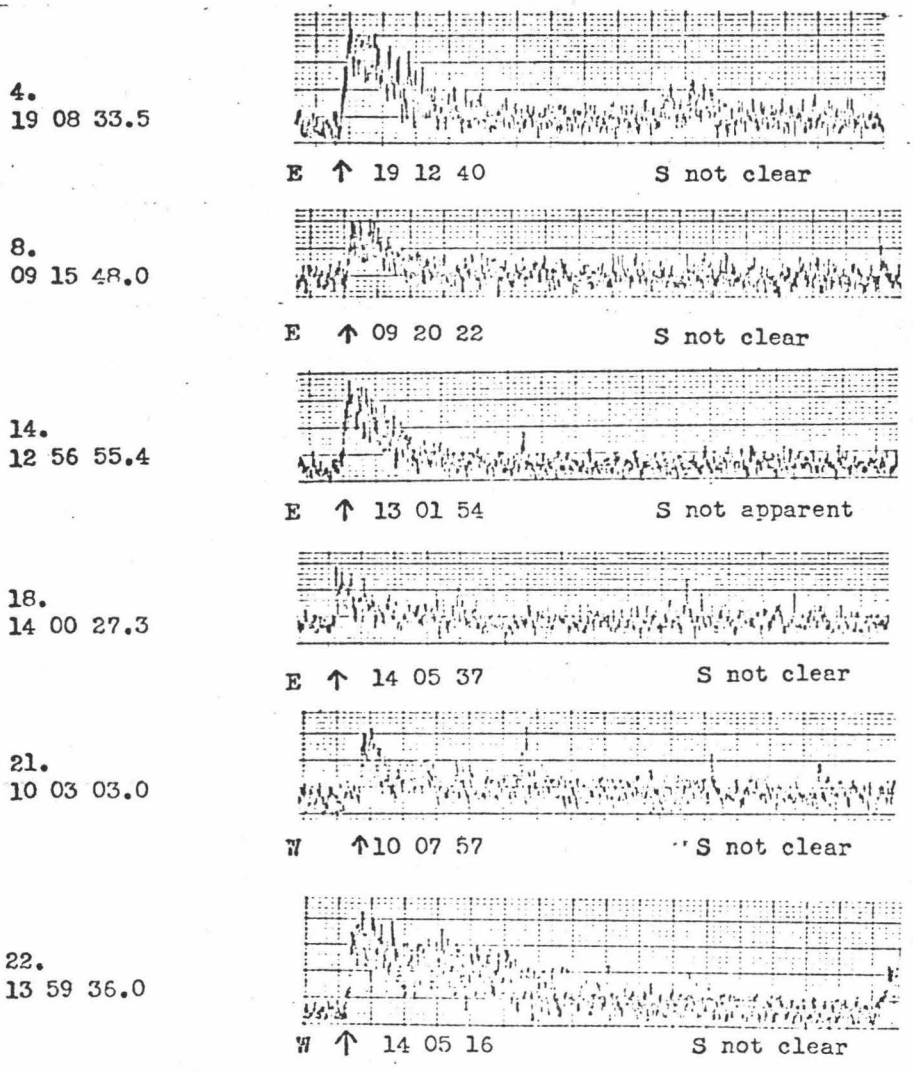

Fig. 8. Observed hydrophone arrivals from events south of 12° north latitude (the time scale is the same as in Fig. 2).

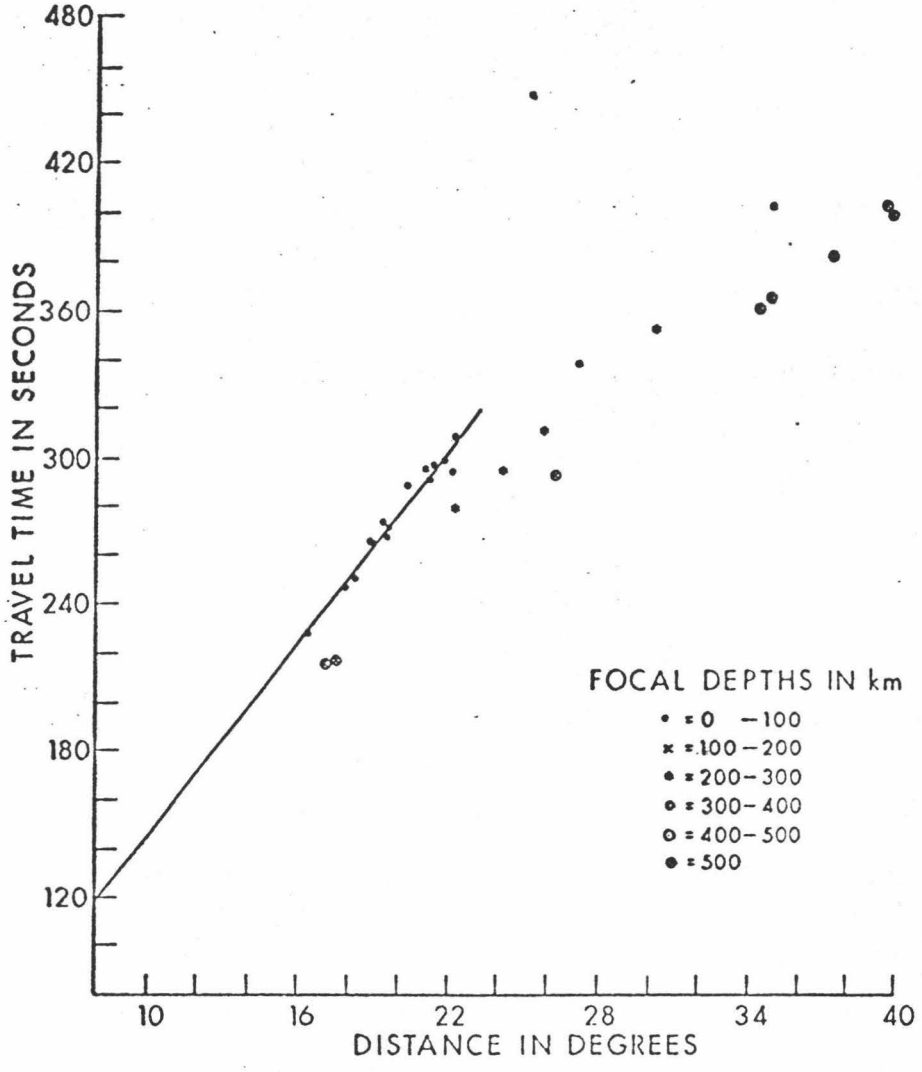

Fig. 9. Travel-time curve for compressional arrivals from events south of 12° north latitude (hydrophone data).

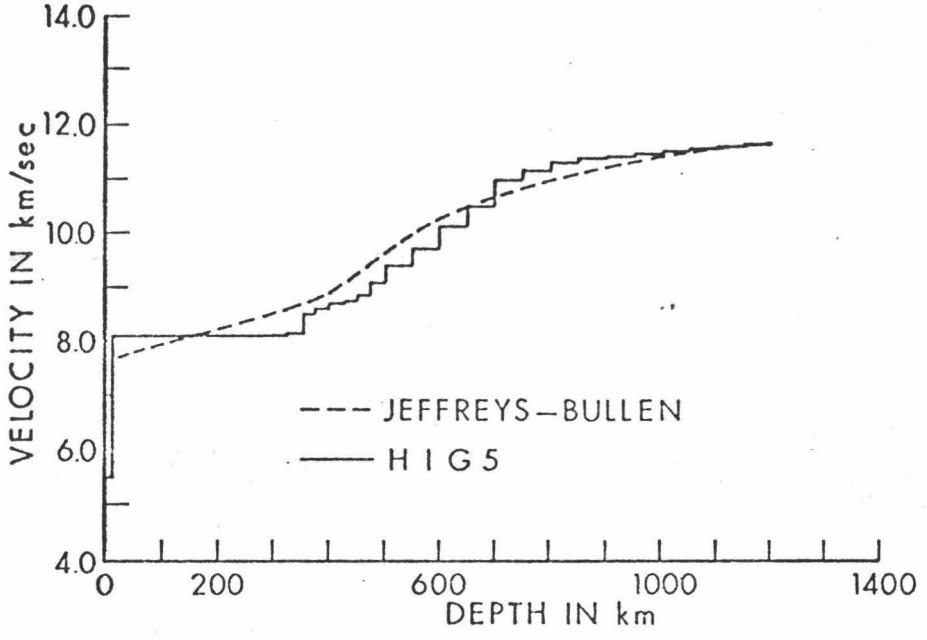

Fig. 10. HIG 5 model for compressional waves south of 12° north latitude (hydrophone data only).

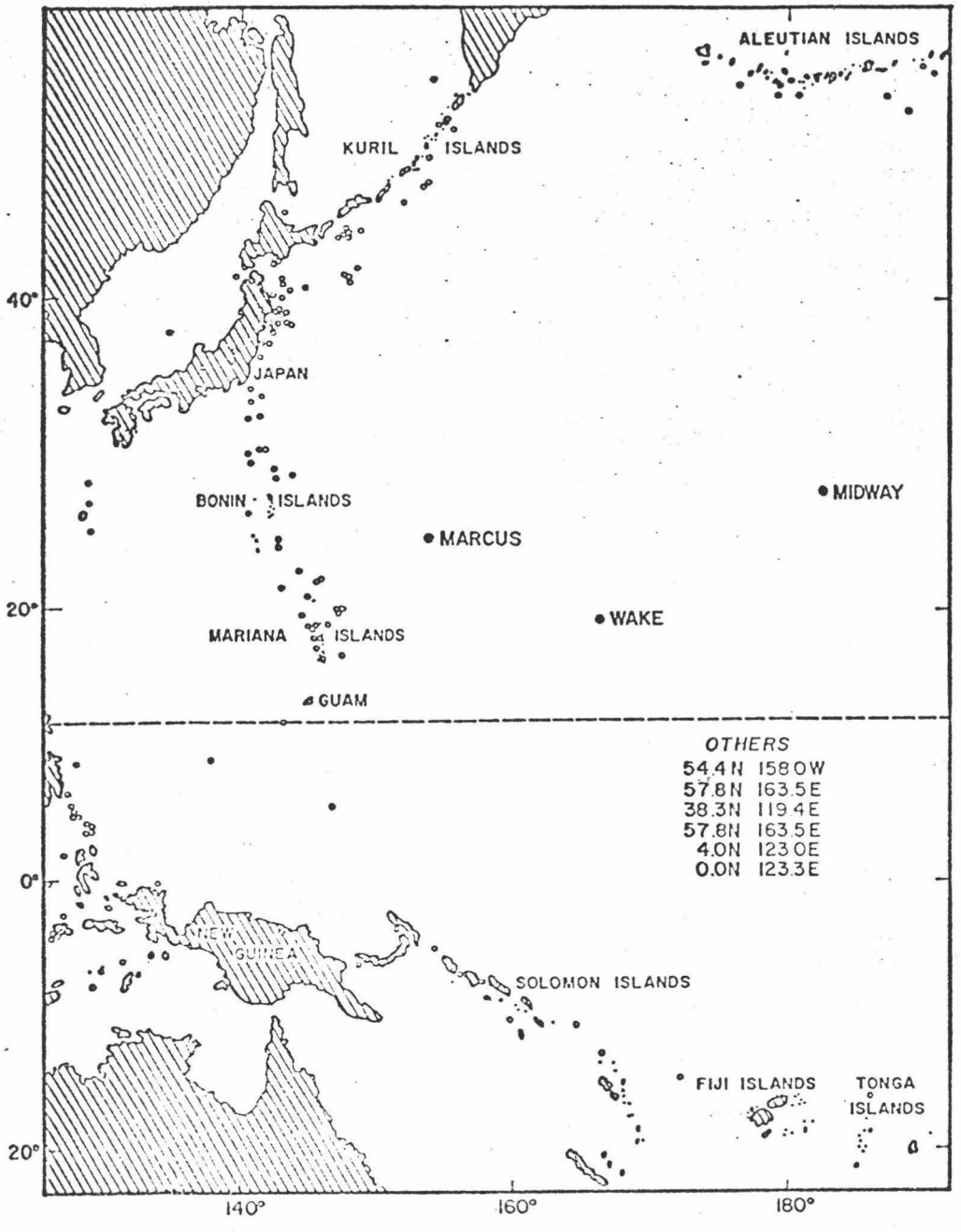

Fig. 11. Epicenter map for seismograph data.

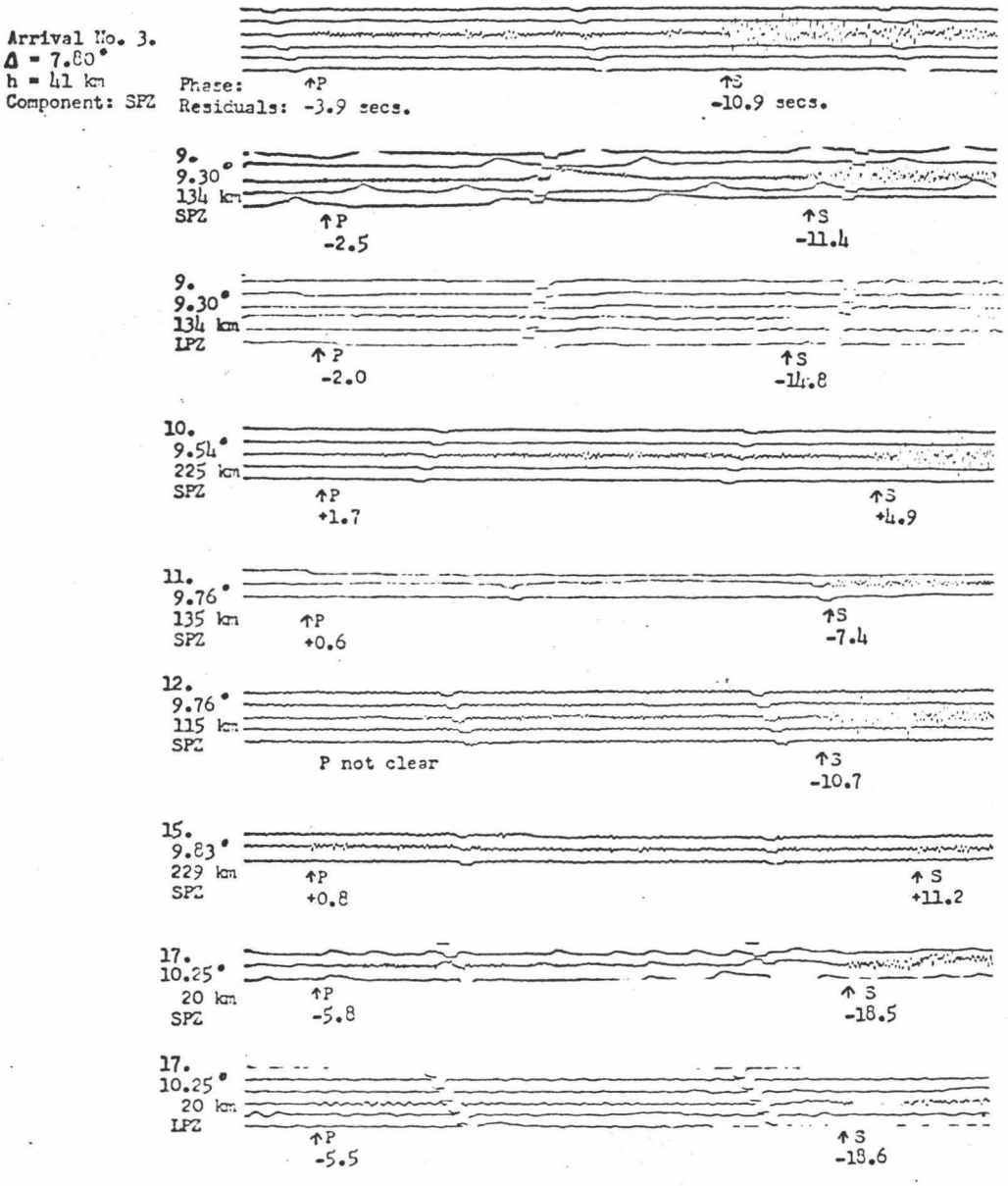

Fig. 12. Observed seismograph arrivals from events north of 12° north latitude (the interval between time marks is one minute).

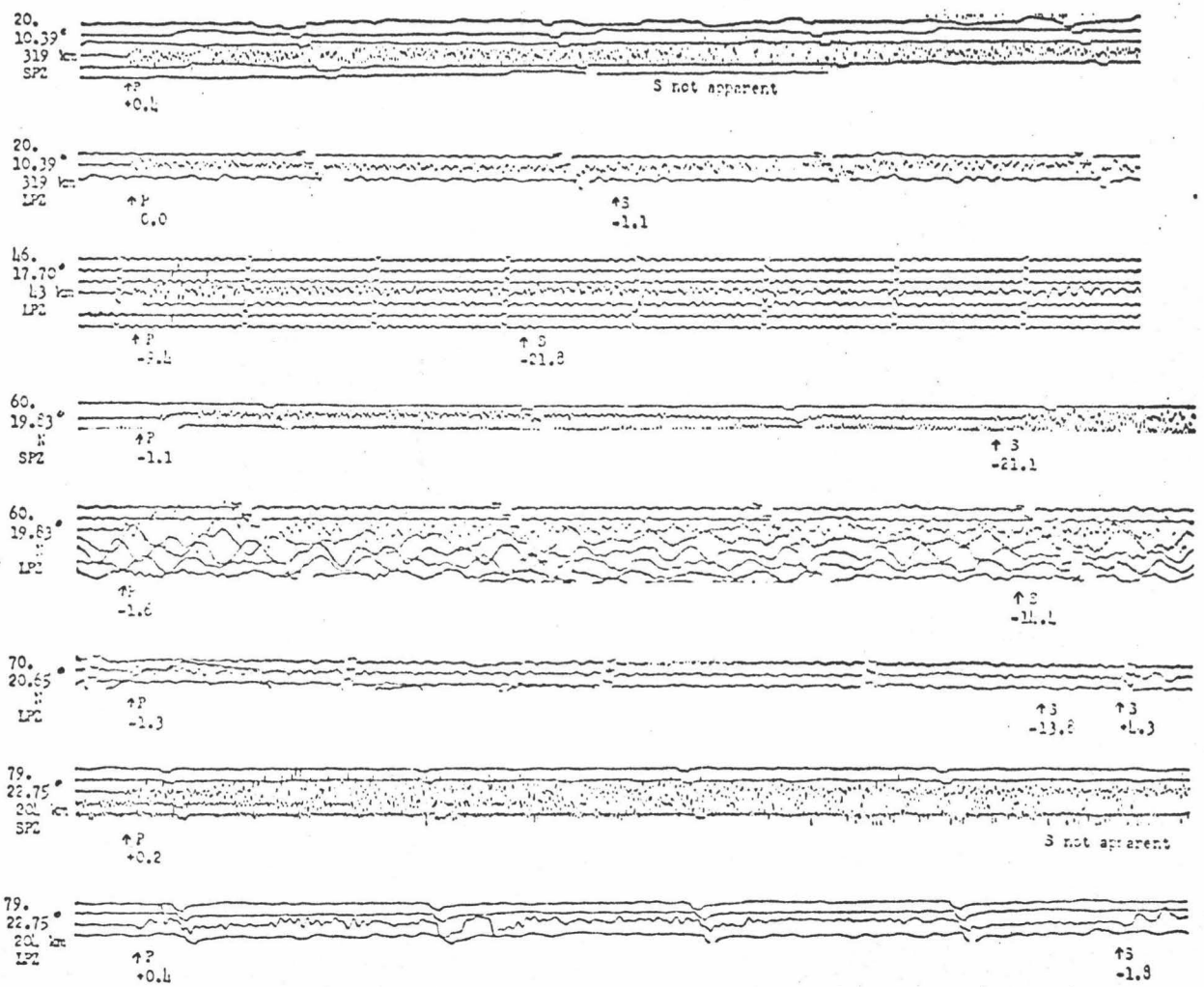

Fig. 12. (continued)

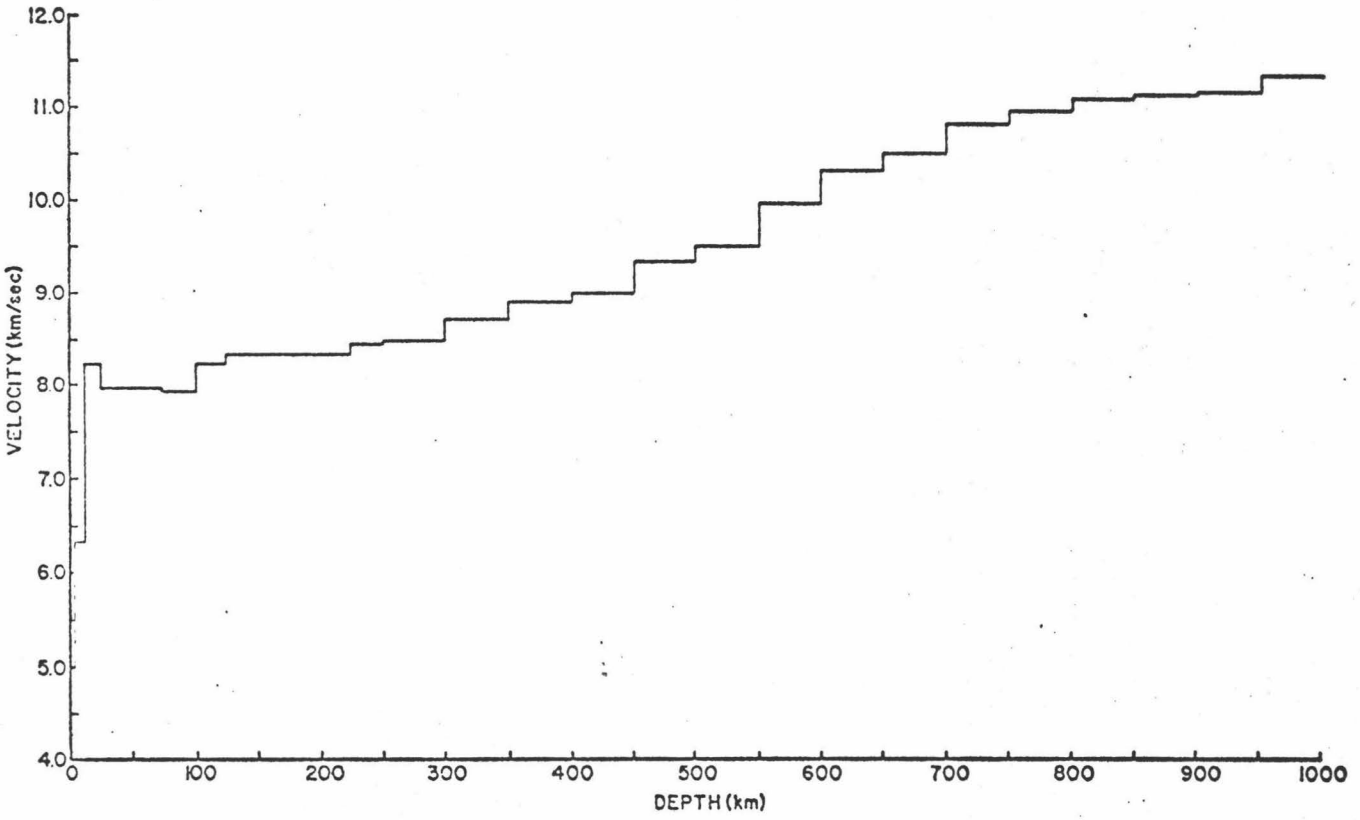

Fig. 13. P velocity distribution for Northwestern Pacific Basin 1 model.

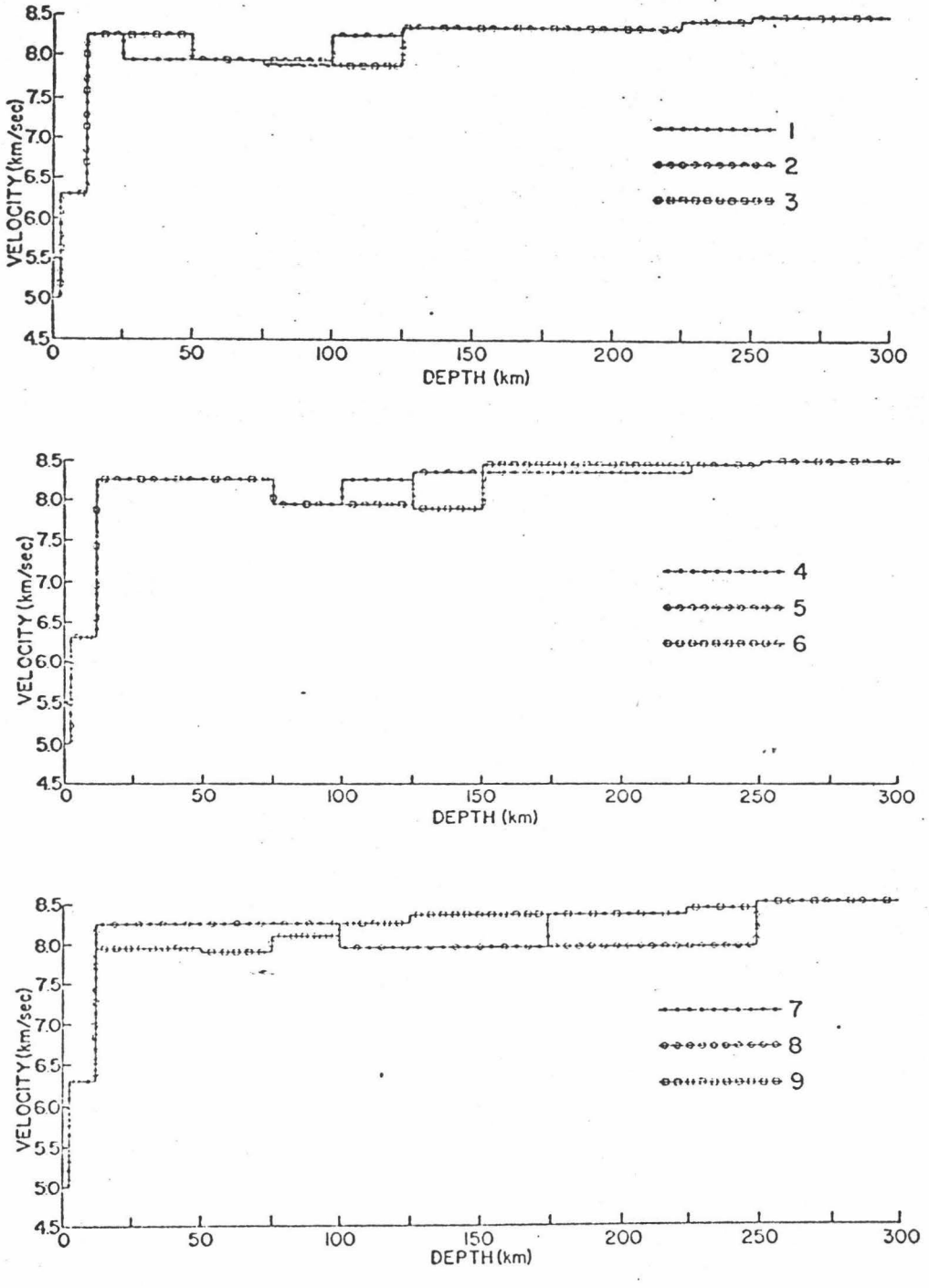

Fig. 14. P velocity distribution for Northwestern Pacific Basin models.

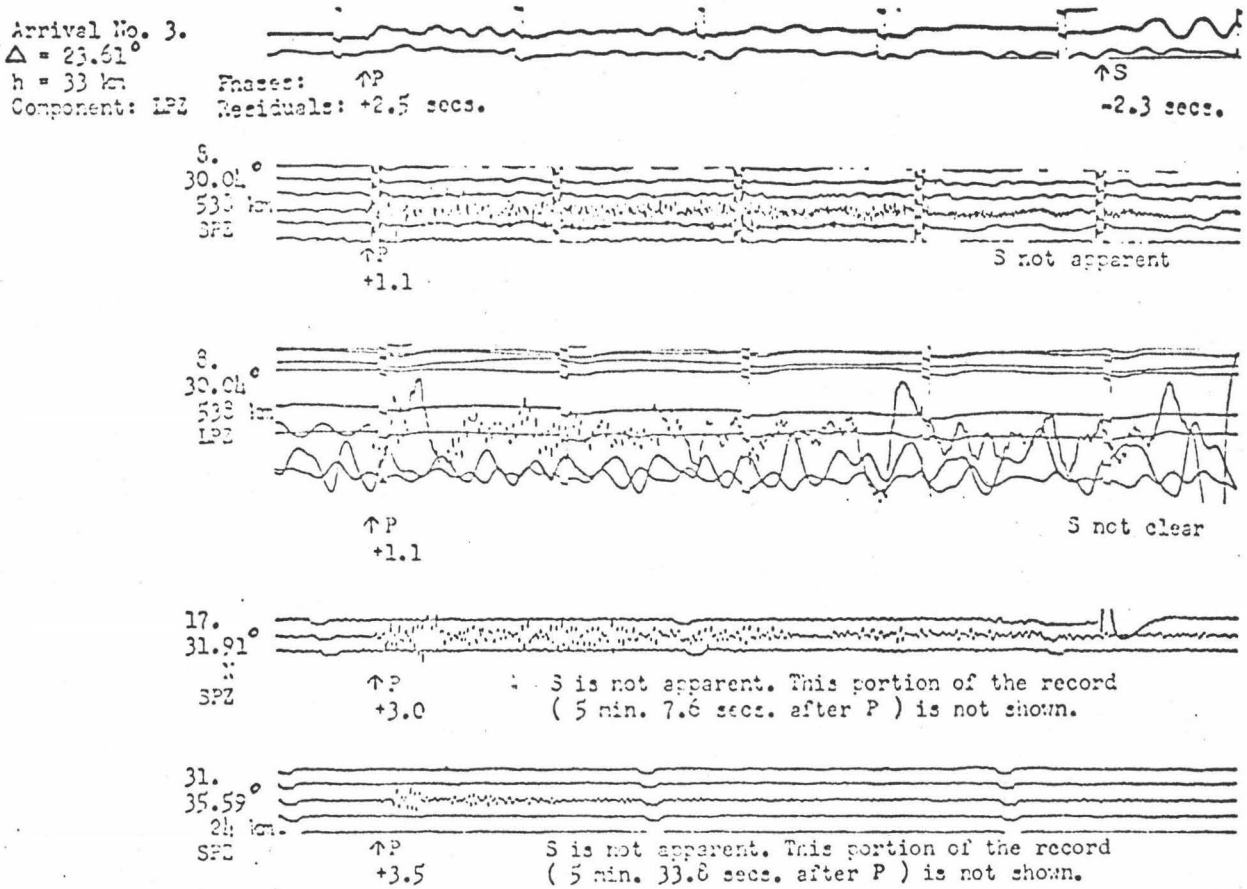

Fig. 15. Observed seismograph arrivals from events south of 12° north latitude (the interval between time marks is one minute).